DISSERTATIONES
GEOGRAPHICAE
UNIVERSITATIS
TARTUENSIS
**85**

BRUNO MONTIBELLER

# Evaluating human-induced forest degradation in different biomes using spatial analysis of satellite-derived data

DISSERTATIONES GEOGRAPHICAE UNIVERSITATIS TARTUENSIS
**85**

DISSERTATIONES GEOGRAPHICAE UNIVERSITATIS TARTUENSIS
**85**

**BRUNO MONTIBELLER**

# Evaluating human-induced forest degradation in different biomes using spatial analysis of satellite-derived data

UNIVERSITY OF TARTU
Press
1632

Department of Geography, Institute of Ecology and Earth Sciences, Faculty of Science and Technology, University of Tartu, Estonia.

This dissertation has been accepted for the commencement of the degree of Doctor of Philosophy in geoinformatics at the University of Tartu on 25th of August, 2022 by the Scientific Council of the Institute of Ecology and Earth Sciences, University of Tartu.

Supervisors: Associate Prof. Evelyn Uuemaa
Institute of Ecology and Earth Sciences
University of Tartu
Estonia

Prof. Ülo Mander
Institute of Ecology and Earth Sciences
University of Tartu
Estonia

Opponent: Dr. Cornelius Senf
Department of Life Science Systems
Technical University of Munich

Commencement: Senate Hall, University Main Building, Ülikooli 18, Tartu, on 6th of December, 2022, at 14.15

Publication of this dissertation is granted by the Institute of Ecology and Earth Sciences, University of Tartu.

ISSN 1406-1295 (print)
ISBN 978-9916-27-031-8 (print)
ISSN 2806-2302 (pdf)
ISBN 978-9916-27-032-5 (pdf)



University of Tartu Press
www.tyk.ee

# TABLE OF CONTENTS

# LIST OF ORIGINAL PUBLICATIONS

This thesis is based on the following publications, which are referred to in the text by Roman numerals:

Published papers are reproduced in print with the permission of the publisher.

I **Montibeller, B.**, Kmoch, A., Virro, H., Mander, Ü., Uuemaa E., 2020. Increasing fragmentation of forest cover in Brazil's Legal Amazon from 2001 to 2017. *Scientific Reports* 10, 5803. https://doi.org/10.1038/s41598-020-62591-x

II **Montibeller, B.**, Jaagus, J., Mander, Ü., Uuemaa, E. 2021. Evapotranspiration intensification over unchanged temperate vegetation in the Baltic countries is being driven by climate shifts. *Frontiers in Forests and Global Change* 4, 663327. https://doi.org/10.3389/ffgc.2021.663327

III **Montibeller**, B., Marshall, M., Mander, U.,Uuemaa, E., 2022. Increased carbon assimilation and efficient water usage may not compensate for carbon loss in European forests. Communications Earth & Environment, 3(1), p. 1–11. https://doi.org/10.1038/s43247-022-00535-1.

Author's contribution to the articles denotes: '*' a minor contribution, '**' a moderate contribution, '***' a major contribution.

| | Articles | | |
|---|---|---|---|
| | I | II | III |
| Original idea | *** | *** | *** |
| Study design | *** | *** | *** |
| Data processing and analysis | ** | *** | *** |
| Interpretation of the results | *** | *** | *** |
| Writing the manuscript | *** | *** | *** |

# LIST OF ABBREVIATIONS

| | |
|---|---|
| BLA | Brazilian Legal Amazon |
| CCI | Climate Change Initiative |
| E-OBS | European Climate Assessment and Dataset |
| ET | Evapotranspiration |
| FAO | The Food and Agriculture Organization |
| FCA | Forest core areas |
| FIRMS | Fire Information for Resource Management System |
| GFC | Global Forest Watch |
| GPP | Gross primary production |
| IPCC | The Intergovernmental Panel on Climate Change |
| LULC | Land use and land cover |
| MK | Mann-Kendall |
| MODIS | Moderate Resolution Imaging Spectroradiometer |
| PPCDAm | Action Plan for the Prevention and Control of Deforestation in the Legal Amazon |
| PRODES | Amazon Deforestation Monitoring Project |
| TS | Theil-Sen slope |
| WUE | Water-use-efficiency |

# 1. INTRODUCTION

Human activities have been the main drivers of direct impacts (e.g., via land use and land cover change) and indirect impacts (e.g., climate change) on the dynamics of terrestrial ecosystems (Nolan et al., 2018; Díaz et al., 2019). The magnitude and intensity of these human impacts depend on the type of human activity (direct or indirect), on the spatial scale, and on the ecosystem's sensitivity (Seddon et al., 2016).

Forest ecosystems are especially affected by human activities (McDowell et al., 2020). The most common human impact on forest ecosystems is deforestation. In this process, the natural forest land use changes to alternatives such as commodity production, shifting agriculture, and forestry (Curtis et al., 2018), and the resulting ecosystem generally cannot provide the original forest's ecosystem services (Xu et al., 2022). Moreover, the remaining standing forests are susceptible to other types of direct or indirect drivers of forest degradation by humans (e.g., forest fragmentation, selective logging, harvesting, reduction of ecosystem services due to anthropogenic climate change) that are known to be (Anderegg et al., 2020a; Bullock et al., 2020) .

The Intergovernmental Panel on Climate Change defines forest degradation as a reduction in biological productivity, reduction of canopy cover, loss of ecological integrity, and loss of carbon stocks (IPCC, 2019). Similarly, the Food and Agriculture Organization's definition of forest degradation is "*changes within the forest which negatively affect the structure or function of the stand or site, and thereby lower the capacity to supply products and/or services*" (FAO, 2011). Differences among these and other definitions combine with the technical limitations of using remote sensing images to detect forest degradation have created challenges for mapping, monitoring, and quantifying this ecosystem change (Gao et al., 2020). A problem that arises from these challenges is that the $CO_2$ emission from forest degradation is often missing from national carbon emission estimates (Assis et al., 2020). However, despite the challenges posed by differences in the definition, researchers have proposed methodologies to investigate and monitor forest degradation at different spatial and temporal scales. For instance, Hansen et al. (2013) mapped $2.3 \times 10^6$ $km^2$ of forest loss (including degradation) across the globe from 2000 to 2012 based on satellite images, with the tropics showing an average annual increase of 2101 $km^2$ for forest loss. Pearson et al. (2017) reported that forest degradation due to selective logging, fuelwood harvesting, and forest fires within tropical and subtropical latitudes was responsible for releasing 2.1 Gt of $CO_2$ per year from 2005 to 2010, which represents 25% of total carbon emission from deforestation plus forest degradation. The changes in climate patterns, such as warmer summer temperatures and increasing frequency or severity of summer drought, are also drivers of forest degradation due to a reduction in forest productivity that results from higher carbon release (Sippel et al., 2017). These results highlight the importance of monitoring forest degradation to correctly evaluate its contribution to greenhouse gas emission (Baccini

et al., 2017) and the essential role of forested areas as nature-based solutions for constraining climate change (Griscom et al., 2020).

In this dissertation, I define *forest degradation* as the result of negative impacts on a forest that compromise or alter the forest's capacity to maintain essential ecosystem services (e.g., carbon assimilation, water cycling, and climate regulation). Given this definition and the abovementioned context, I evaluate two processes related to forest degradation: (i) fragmentation of tropical forest cover and (ii) changes in forest evapotranspiration and the carbon cycle in undisturbed forest areas. I treat forest fragmentation as a direct human-induced forest degradation since it is most strongly related to deforestation. On the other hand, I consider changes in evapotranspiration and carbon cycles to be indirect human-induced forest degradation since the changes in these ecosystem processes relate most strongly to the effects of anthropogenic climate change. I used satellite-derived data and spatial analyses to assess the impacts of forest degradation to fill gaps in the research literature by means of three different case studies (**articles I to III**), which I will discuss in the next three sections.

## 1.1. Forest fragmentation (Article I)

Forest fragmentation refers to the division of forest areas into separate patches and results from reduction in the size of intact forest areas through deforestation (Laurance et al., 2011; Haddad et al., 2015). The forest degradation related to fragmentation increases forest fire susceptibility (Alencar et al., 2015; Silva et al., 2018), tree mortality (Buras et al., 2018), and carbon emission, which are all direct results of the edge effects created by the fragmentation (Chaplin-Kramer et al., 2015; Brinck et al., 2017; Fischer et al., 2021). In countries like Brazil, with large carbon stocks in tropical forests and a history of deforestation to convert these areas into cattle farming and soybean production areas (Gollnow et al., 2018), the carbon emission from the edges of fragmented forest was about 30% ($42 \pm 7.67$ Tg C year$^{-1}$) of the carbon loss from deforestation (Silva et al., 2020). Thus, reducing deforestation rates would not only decrease carbon emission related to complete removal of the forest but potentially also decrease the carbon emission from forest degradation (e.g., due to the edge effects). In the present thesis, I analyse forest fragmentation as one aspect of direct human-induced forest degradation in the Brazilian Amazon. The region is the world's largest area of intact tropical forest (Potapov et al., 2017) and has faced intense pressure from land use and land cover change since 1970 (Brown et al., 2016).

To halt the deforestation that leads to forest fragmentation in the so-called Brazilian Legal Amazon (i.e., a specific socio-geographic division of Amazon region in Brazil; BLA), the Action Plan for the Prevention and Control of Deforestation in the Legal Amazon (PPCDAm) (República, 2004) and the Soy Moratorium programs (Rudorff et al., 2011; Gibbs et al., 2015) were launched in 2004 and 2006, respectively. The programs played an important role in reducing the deforestation of primary forest in the BLA from 27.8 km$^2$ in 2004 to 4.6 km$^2$

in 2012 according to data from PRODES, the national deforestation program (INPE, 2016). However, even though PRODES data was essential to support efforts to reduce the deforestation rate, it only identified the subset of deforestation that results from complete removal of the forest cover in areas larger than 6.25 ha within the BLA primary forest cover (INPE, 2016; Kalamandeen et al., 2018). Moreover, PRODES does not include data on deforestation in other forest types (e.g., secondary forest, savannah, shrubland) or other types of forest disturbance that result in forest degradation rather than complete deforestation (e.g., illegal selective logging and fire). Therefore, despite its importance in monitoring deforestation rates, limitations of the PRODES data mean that it cannot support a complete assessment of the forest degradation process in the BLA. On the other hand, high-resolution data such as the Global Forest Change (https://www.globalforestwatch.org) dataset can improve the assessments of forest dynamics in the BLA. This data consists of annual maps that identify areas of forest loss greater than 0.09 ha and that account for different types of forest disturbance (e.g., fire, selective logging, deforestation). Multiple studies have used Global Forest Change and PRODES data to evaluate either deforestation (Rosa et al., 2012; Kalamandeen et al., 2018) or the spatial structure of the remaining forest cover in the BLA (Vedovato et al., 2016; Taubert et al., 2018). However, no study has yet provided a long-term, high-resolution, wall-to-wall analysis that combines forest loss and forest fragmentation in the BLA.

To provide a better understanding of the forest degradation process that results from forest loss and the dynamics of forest fragmentation in the BLA, I defined three research questions: (i) How did the trends in forest loss influence the forest fragmentation process from 2001 to 2017? (ii) Did the forest fragmentation increase or decrease over time? (iii) Did forest fragmentation differ between primary and non-primary forests? I hypothesized that despite the observed decrease in forest loss, especially from 2004 to 2012, the fragmentation of the remaining forest cover did not decrease due to an increase in the dispersion of forest loss throughout the BLA (Kalamandeen et al., 2018).

## 1.2. Changes in temperate forest evapotranspiration (Article II)

Human-driven land use and land cover (LULC) change is a major factor that exacerbates the effects of climate change and can, itself, cause localized climate change at different spatial scales (Findell et al., 2017; Ceccherini et al., 2020; Sy and Quesada, 2020). The changes in climate patterns, in turn, can directly affect the functions of other ecosystems that have not faced LULC changes, such as forests. For instance, warming temperatures can lead to forest degradation when they increase the forest's susceptibility to fire (Holden et al., 2018; Abram et al., 2021). Degraded forest areas usually show a decrease in important ecosystem services that are directly linked to complex land–atmosphere interactions (Alkama and Cescatti, 2016). An important ecosystem service affected by climate

change is the evapotranspiration (ET) process, which plays an important role in hydrological cycles (Zhang et al., 2016).

Although multiple studies have used remote sensing and modelling approaches to estimate ET and analyse the effects of LULC change on ET at different spatial scales (Dias et al., 2015; Spera et al., 2016; Poon and Kinoshita, 2018; Paca et al., 2019; dos Santos et al., 2020; Liu et al., 2021), there have been fewer studies of how ET has changed in undisturbed LULC types, such as forest. ET changes in undisturbed areas are most likely to be driven solely by changes in climate (Li et al., 2017). Research has revealed that warming temperatures decreased ET in semi-deciduous tropical forests (Vourlitis et al., 2014) but that temperate forests showed an increase in ET due to the longer growing season induced by warming temperatures (Gaertner et al., 2019). These studies focused only on the annual ET and did not simultaneously account for the spatial variation of ET and its changes over time. This makes it difficult to identify the trade-offs that occur between monthly and seasonal time scales. Therefore, in this dissertation, I analysed the spatial and temporal changes of ET as an indicator of the effects of the forest degradation induced by climate change on the provision of this important ecosystem service.

In this context, I defined two research questions to better understand how ET changes spatially and temporally in undisturbed forest: (i) What are the spatial and temporal patterns of temperature, precipitation, and ET throughout the Baltic countries? (ii) How has the ET of undisturbed forest areas changed in this region? I defined the Baltic region as my study area due to the observed shifts in its climate patterns from 1951 to 2015, with gradual warming and a slight trend of increasing precipitation (Jaagus et al., 2017). Moreover, no intense LULC change occurred in the region during the study period, thereby allowing a focus on climatic effects. I hypothesised that despite the lack of significant LULC change in the region, the ET rates of forest have changed as an adaptation to the changing climate of the Baltic countries (Jaagus et al., 2003). I have used the term *climate shift* throughout the thesis instead of *climate change* because the period under study is shorter than the recommended duration for climate change studies (Seneviratne et al., 2012).

## 1.3. Changes in forest carbon assimilation across undisturbed forest areas (Article III)

Forest degradation can reduce photosynthetic carbon uptake (Anderson et al., 2018), which is the main driver of carbon and water fluxes between forest ecosystems and the atmosphere (Aragão, 2012; Ellison et al., 2017; Pugh et al., 2019; Harris et al., 2021). During photosynthesis, atmospheric $CO_2$ is assimilated and stocked as biomass, whereas the roots recycle water from the soil and trees release it into the atmosphere as water vapour. Forest ecosystems can sequester up to 12% of anthropogenic $CO_2$ emission and return up to 40% of the local precipitation to the atmosphere (Schlesinger and Jasechko, 2014). Therefore, forest

ecosystems play an important role in mitigating human $CO_2$ emission and sustaining aspects of the water cycle such as precipitation at different spatial scales (Makarieva et al., 2013; Grassi et al., 2017; Staal et al., 2018).

The quantity of $CO_2$ assimilated by an ecosystem is defined as gross primary production (GPP) and the water vapour that is lost through a combination of evaporation and transpiration is defined as evapotranspiration (ET). The dynamics of these two variables are directly affected by environmental conditions, which in turn are directly affected by climate (Hatfield and Dold, 2019; Zohner et al., 2020). Warmer temperatures during the spring and autumn under global warming result in a longer growing season that leads to increased GPP in terrestrial ecosystems in both seasons (Keenan et al., 2014). In addition, warmer summers offset the GPP gain during spring and autumn due to an increase in respiration, which releases carbon back into the atmosphere. The warmer temperatures can also increase ET by increasing both evaporation and transpiration rates (Schlesinger and Jasechko, 2014), which, in turn, decreases the soil water availability (Palareti et al., 2016; De Kauwe et al., 2019; Gaertner et al., 2019; Harrison et al., 2020; Lian et al., 2020). These climate-driven alterations in the dynamics of GPP and ET can be characterized as indirect human-induced forest degradation.

Several studies have used field data to evaluate the change of forest GPP, ET, and water-use efficiency (WUE = GPP/ET; i.e., the quantity of carbon assimilated per unit of water released) (Tang et al., 2014; Knauer et al., 2017; Fu et al., 2020). Multiple studies have instead used Earth observation data to parameterize models that estimate the three variables (Wolf et al., 2016; Cheng et al., 2017; Buermann et al., 2018). Earth observation data facilitates spatial and temporal analyses over large areas and long periods to provide a complete picture of the GPP, ET, and WUE trends over large forest areas at high spatial resolution. Spatial and temporal analyses let us identify the forest areas that show trends of increasing or decreasing GPP, ET, and WUE, and support investigations of the environmental drivers behind the trends, such as an increased leaf area index and a rising atmospheric $CO_2$ concentration (Wolf et al., 2016; Cheng et al., 2017; Buermann et al., 2018). Moreover, these studies have also provided insights into the temporal and spatial compensation of GPP, which results from offsetting GPP increases and decreases in different areas or periods (Wolf et al., 2016; Cheng et al., 2017; Buermann et al., 2018). GPP compensation occurs (for example) when a spring GPP increase offsets a summer GPP decrease (i.e., temporal compensation) or when one forest area shows a GPP increase that offsets the GPP decrease in another forest area (i.e., spatial compensation). Environmental variables (e.g., soil water availability, vapor-pressure deficit) and biotic variables (e.g., phenology, seasonality) can also be drivers that influence GPP compensation (Wolf et al., 2016; Buermann et al., 2018).

Although several studies have provided insights into the GPP dynamics of forests (Cheng et al., 2017; Van Schaik et al., 2018), no high-resolution studies have focused on whether the trade-off between GPP increases and decreases resulted in a net GPP loss or gain in forested areas. GPP loss occurs when a GPP increase is not enough to compensate for a GPP decrease (e.g., the increased

spring or autumn GPP does not compensate for decreased summer GPP) whereas GPP gain occurs when a GPP increase compensates for a GPP decrease (e.g., increased spring or autumn GPP offsets a decreased summer GPP). Most GPP compensation studies were based on seasonal GPP averages throughout a study region (Wolf et al., 2016) or on the outputs of GPP models with coarse spatial resolution (Sippel et al., 2017; Buermann et al., 2018). This limits our ability to understand intra-annual and spatial variation of GPP over large areas and the identification of degraded forest areas. Moreover, there is no clear understanding of whether an increase of seasonal forest GPP is accompanied by an increase in WUE (Wang et al., 2018; Jiang et al., 2019). Few studies reported that GPP and WUE increased simultaneously due to the decrease in ET caused by stomatal closure, which is induced by an elevated atmospheric $CO_2$ concentration or decreased water availability (Wang et al., 2018; Jiang et al., 2019). Stomatal closure occurs to control the $CO_2$ uptake for photosynthesis and to reduce water loss. WUE studies have been mostly based on eddy-covariance data that are acquired at specific forest sites (Dekker et al., 2016; Guerrieri et al., 2019). Such studies cannot identify large-scale variation in forested areas and variation over long time periods. Analyses of forest GPP compensation and WUE dynamics in large areas of undisturbed forest are important to evaluate the impacts of climate change on these variables. Furthermore, such analyses can potentially identify degraded forest areas that require management strategies that will enhance net carbon assimilation (Schelhaas et al., 2015; Law et al., 2018; Griscom et al., 2020).

My thesis aims to fill some of these gaps in the literature by investigating GPP, ET, and WUE of undisturbed temperate-zone forest core areas (i.e., the central area of forest patches; FCAs) in Europe. I used FCAs to avoid any potential bias in the analysis due to edge effects, which can alter the carbon and water dynamics of trees growing near forest edges (Silva et al., 2020). To support this investigation, I defined three research questions: (i) What were the spatial and temporal trends of GPP, ET, and WUE in FCAs across Europe from 2000 to 2020? (ii) Has the temperature-driven increase in GPP during spring and autumn been accompanied by an increase in WUE? (iii) Does a given FCA that shows a mixture of GPP decreases and increases throughout the year show an annual GPP gain or loss? (That is, did an increased spring and autumn GPP offset a decreased summer GPP?) I hypothesised that (i) the spring and autumn GPP increase would not be accompanied by increased WUE in some of the FCAs due to a widespread increase of ET that has been observed in Europe (Teuling et al., 2019); and (ii) GPP compensation within and across seasons would not necessarily occur in a given FCA because of different forest responses to the varying environmental conditions across the large study area (Wolf et al., 2016; Buermann et al., 2018).

# 2. MATERIAL AND METHODS

## 2.1 Evaluation of forest fragmentation based on remote sensing derived data and spatial analysis (Article I)

To evaluate the spatio-temporal patterns the forest loss and forest fragmentation dynamics in the Brazilian Legal Amazon, a baseline forest cover map for the year 2000 and annual forest loss maps from 2001 to 2018 were used. The identification of the areas with increasing or decrease trends in the forest loss and fragmentation processes was performed for the entire BLA, but also for areas within and outside indigenous reserves and conservation units, and for areas within primary and non-primary forests.

### 2.1.1 Study area – Brazilian Legal Amazon

The Brazilian Legal Amazon region includes nine Brazilian states in the Amazon basin and covers ~5.2 × $10^6$ $km^2$ (Figure 1). It includes vegetation types from three different biomes: i) Amazonia biome, ii) Cerrado biome and iii) Pantanal biome. The Amazonia biome is composed by moist broadleaf forest whereas Cerrado biome is composed by tropical savanna and grasslands. Pantanal biome is covered by a mix of vegetation types, including woodland, savanna and grasslands, which are flooded during the rainy season.

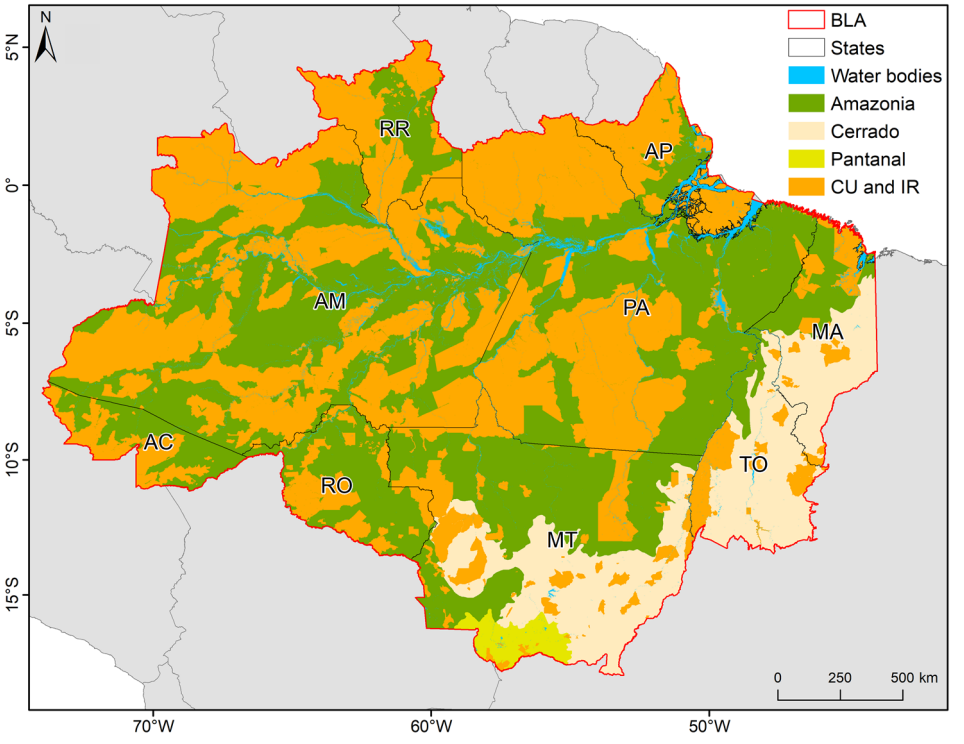


**Figure 1**. Map of the study area – Brazilian Legal Amazon (BLA). The Brazilian are states: Acre (AC), Amazonas (AM), Amapá (AP), Maranhão (MA), Mato Grosso (MT), Pará (PA), Rondônia (RO), Roraima (RR), and Tocantins (TO). Amazonia, Cerrado and Pantanal are the biomes within BLA. The orange colors areas are conservation units (CU) and indigenous reserves (IR).

### 2.1.2 Research data

*Forest cover and forest loss data for the BLA*

Forest cover and forest loss data provided by Global Forest Chage initiative and developed by Hansen et al (2013) were used to assess the spatio-temporal patterns of forest fragmentation and loss in the BLA from 2001 to 2017. The forest cover data indicates the percentage of tree cover within the 30×30 meter Landsat pixel in 2000. The forest loss data indicates the Landsat pixels with significant forest disturbance (e.g., fire degradation, wind throw, selective log) or with complete removal of the tree cover on annual basis.

A binary mask indicating areas of forest/no-forest was created for the year 2000 using a tree cover threshold of 30% (>=30% forest; <30% no-forest). Based on this mask, all forest loss pixels from 2001 to 2017 that overlapped the no-forest areas were eliminated from the analysis. Then, the updated annual forest loss data was used to derive annual forest cover masks as described in the following schema:

$$FC_{2001} = FC_{2000} - FL_{2001};\ FC_{2002} = FC_{2001} - FL_{2002};\ \ldots\ FC_{2017} = FC_{2016} - FL_{2017}$$

where FC is the forest cover and FL is the forest loss in the respective year. The lack of annual forest regrowth data was not a limitation for the fragmentation analysis as the regenerated forest areas are often logged and replaced by other land use and land cover types

*Primary and non-primary forest mask*

The PRODES primary forest cover mask was used to separate primary and non-primary forest areas in the BLA. This enabled to identify potential shifts in the forest loss process from primary to non-primary forest after the implementation of anti-deforestation initiatives.

*Conservation units and indigenous reserves data*

The limits of conservation units and indigenous reserves were acquired from the Environmental Ministry of Brazil and were used to define which forest cover and forest loss pixels belonged to these areas. The use of these limits allowed to divide the analysis into four categories: (i) conservation units based on integral protection, (ii) conservation units based on sustainable use, (iii) indigenous reserves and (iv) regions with overlapping categories.

*Active fire data*

The Fire Information for Resource Management System (FIRMS) active fire product was used to estimate the area of forest loss caused by fire. Annual FIRMS fire points were overlaid with the forest loss patches (polygons) of the respective year. The area of these forest loss patches was summarized per year, obtained then, the total area of forest loss potentially caused by fire.

### 2.1.3 Research methods

*Forest cover and forest loss metrics*

The forest loss dynamics were investigated based on the size distribution of forest loss patches annually. Eight patch size groups were defined based on previous studies: <1 ha; ≥1 and <6.25 ha; ≥6.25 ha and <50 ha; ≥50 ha and <100 ha; ≥100 ha and <200 ha; ≥200 ha and <500 ha; ≥500 ha and <1000 ha; and ≥1000 ha. For each year from 2001 to 2017, the total forest loss area was estimated for each size group. The forest fragmentation dynamics were estimated based on the additional number of forest fragments compared with the prior year (e.g., number of fragments in 2001 – number of fragments in 2000 = number of additional fragments in 2001).

To analyse the spatial distribution of forest loss, a 10 km × 10 km grid (fishnet) was created. For each of the 51 220 grid cells, the area of the original forest cover in 2000 and the total forest loss per year were calculated. Based on the forest cover and forest loss values, the percentage of forest loss in relation to the original forest cover was calculated for each grid cell as follows:

$$\text{forest loss in the respective year/forest cover in 2000} \times 100\%$$

Landscape metrics of forest loss and forest cover were calculated for each grid cell: number of patches, mean patch size and edge density (edge length per unit area). The landscape metrics were also calculated for areas within and outside of conservation units and indigenous reserves, and for primary and non-primary forest areas.

*Temporal trend analysis*

The non-parametrical Mann-Kendall statistical test was used to identify the increase or decreasing trends of each landscape metric calculated previously. The test was applied for each grid cell using the time series values of the landscape metrics. We used a confidence interval of 90% which is aligned with the mentioned cluster analysis. The Mann-Kendal test calculation was performed using the "trend" package for the R software.

## 2.2 Remote sensing derived data and spatial analysis to evaluate evapotranspiration over vegetation areas in the Baltic countries (Article II)

The evapotranspiration dynamics over vegetation areas in the Baltic countries were assessed based on its trends from 2000 to 2018. These trends were calculated over unchanged forest areas.

### 2.2.1 Study area – Baltic countries

The Baltic countries – Estonia, Latvia and Lithuania – encompass an area of $175 \times 10^3$ km$^2$ in the north-eastern Europe (Figure 2). With an annual mean temperature of 5.5 to 6.5°C and annual precipitation varying from 600 to 750mm, the climate in the region is classified as humid continental (Dfb) according to Köppen climate classification. However, the region has faced shifts in the precipitation and temperature patterns. The precipitation increased during the winter months of November to March (also in June) whereas annual mean temperature increased by 0.3 to 0.4 K per decade from 1950 to 2015 (Jaagus et al., 2017).

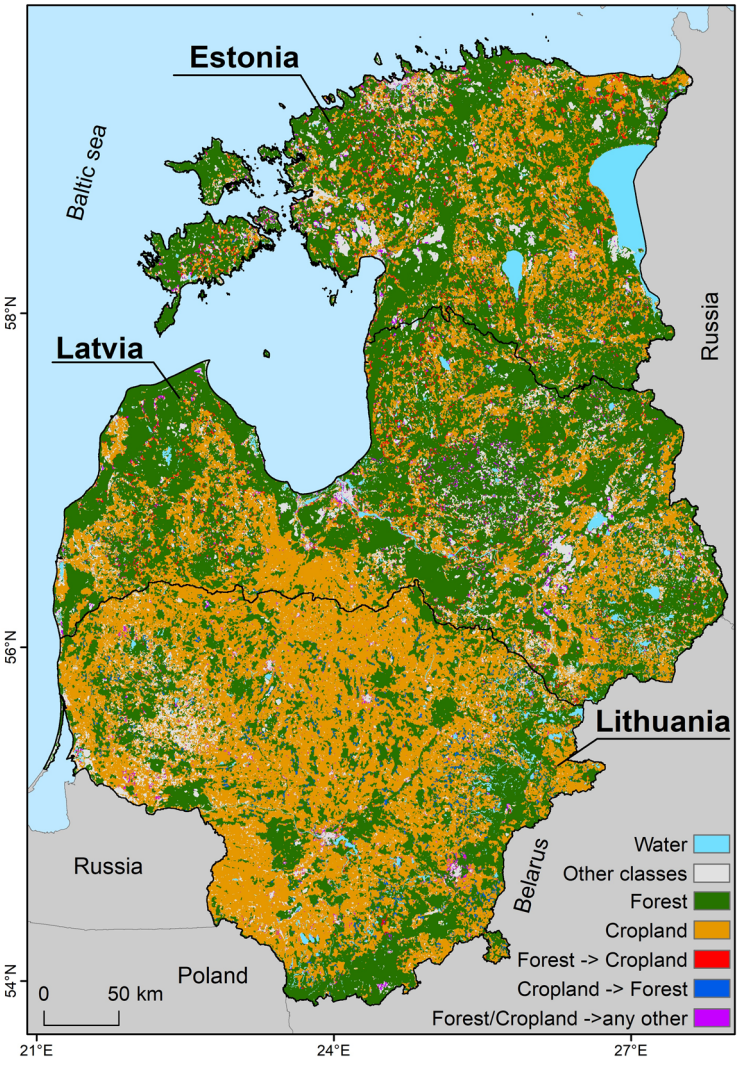


**Figure 2**. Changes in the areas of forest in the Baltic countries from 2000 to 2018.

### 2.2.2 Research data

*Precipitation and temperature data*

Daily precipitation and daily mean temperature data was acquired from the European Climate Assessment and Dataset (E-OBS) (Cornes et al., 2018). Both variables are available at gridded format with a spatial resolution of 0.1° (~10km). The daily values were aggregated into monthly, seasonal and annual values. For precipitation, the daily values were summed according to the time scale whereas for temperature, the mean value was calculated to each time scale.

*Evapotranspiration Data*

The evapotranspiration (ET) data for the study region was acquired from the recently developed MODIS MOD16A2GF product. This product provides ET values ($kg/m^2$) for every 8-days periods within a year with a spatial resolution of ~500 meters. All MOD16A2GF 8-days composites from January 2000 to December 2018 were acquired for the analysis. As the analysis of ET trends were based on monthly, seasonal and annual time scales, the 8-days composites were aggregated into monthly values by calculating the mean of the composites within each month and then multiplied by the number of days in the respective month. The seasonal and annual values were retrieved by aggregating the monthly values. These aggregations were always performed for each MODIS pixel individually and the original $kg/m^2$ units was converted to mm (at a rate of 1 $kg/m^2$ for 1 mm) to align with previous studies. The 8-days ET composites of December, January and February were not used in the analyses due to: i) the lack of composites in January and February of 2016; ii) many pixels of composites within winter months of other years showed with negative values, and this would have resulted in the exclusion of many pixels since only pixels that had plausible values for the whole period were used in the analysis; iii) ET rates in winter are low and the values are negligible, therefore studies have mainly used only the months of the growing season; iv) the non-stratified ET analysis by forest type and as deciduous and evergreen forest are present in the region, the ET rates analysis would be bias since some forest types loses or maintain the leaves.

*Land use and land cover data*

The annual CCI land use and land cover (LULC) product (version 2.0.7) was used to identify the unchanged forest areas over the Baltic countries. These unchanged areas were identified by using the CCI products for the years from 2000, 2005, 2010, 2015 and 2018. Only the unchanged forest areas were used in the analysis.

### 2.2.3 Research methods

*Spatial analysis*

The ET analyses were only performed for the MODIS pixels that had >50% of its area covered by the unchanged forests. To remove any potential bias from the forest edges, a 1km inward buffer as created from the border of the unchanged areas of this land cover type and removed from the analysis. Additionally, MODIS pixels with <50% of its area covered by forest were also excluded from the analysis. Based on that, the ET trends analysis were applied only for the MODIS ET pixels that had core forest areas as the major LULC type. A total of 15359 MODIS ET pixels covered with forest were suitable for the trend analysis.

*Trend analysis*

Similarly to the previous forest fragmentation analysis, the Mann-Kendal (MK) test was used to identify the MODIS ET pixels with significant temporal trends (increase, decrease or no trend). However, the confidence level used was 95% ($p < 0.05$) instead of 90%. The MK was also applied in the temperature and precipitation gridded data.

The Sen's slope (SS) value was used in combination with the MK test to estimate the magnitude of changes in each one the three variables analysed (ET, precipitation and temperature). The median slope value of all pairwise points combination in the time series is used to determine the magnitude of change. Both trend and magnitudes were calculated at pixel scale and at monthly, seasonal and annual timescales. The calculations were performed using the package "wql" available on R software.

## 2.3 Remote sensing-derived data and spatial analysis to evaluate gross primary production and water-use-efficiency changes over unchanged forest (Article III)

### 2.3.1 Research data

*Forest cover and forest disturbance data derived from remote sensing images*

To retrieve the unchanged forest cover area for whole Europe, annual forest disturbances maps from 1986 to 2020 were overlaid with a base forest cover map from 1985 (Senf and Seidl, 2020). All forest areas that faced any type of disturbance from 1986 to 2020 were removed. Therefore, all unchanged forest areas remained were at least 34 years old. The forest edges of the unchanged forest map were also removed to avoid any potential bias in the analysis due to the edge effect. These edges were removed by applying a 500-m inner buffer. The remaining forest areas were named forest core areas (FCA). As the unchanged FCA map

covered the entire Europe, it includes forest types ranging from boreal conifers in the north to deciduous broadleaf trees in the south. However, due to the lack of high-resolution data describing forest types, the analysis was not stratified by forest types.

*Evapotranspiration and gross primary production data from remote sensing*

The MODIS MOD16A2GF and MOD17A2HGF products (version 6) were used as input for evapotranspiration (ET) (Mu et al., 2011) and gross primary estimations (GPP) (Running et al., 2004; Zhao et al., 2005) respectively. Both products provide GPP and ET values at 500-m spatial resolution and are available on https://lpdaacsvc.cr.usgs.gov/appeears/. All 8-days gap-filled composites images from 2000 to 2020 were downloaded for the analysis. However, only composites from March to November of these years were used. The ET composites represent the sum of ET (kg H2O/$m^2$) while the GPP composites represent the sum of GPP (kg C/$m^2$) over the 8-days period. To retrieve the monthly values of ET and GPP, the mean of the 8-days composites within the respective month was calculated and multiplied by the number of days in the month. Only MODIS pixels of both products that showed continuous time series for both variables (ET and GPP) were used for the analysis. The water-use-efficiency was then calculated as the ration between GPP and ET (WUE=GPP/ET)

### 2.3.2 Research methods

*Spatial analysis*

The monthly GPP, ET and WUE trends were only calculated for the MODIS pixels that had >50% (12.5ha) of their area covered with FCA to increase the signal to noise ratio. A total of 185839 pixels were analysed, covering 360150 ha of FCA.

*Trend Analysis*

The Theil-Sen slope (TS) values was used to estimate the magnitude of changes of each variable (GPP, ET and WUE) on monthly basis (Marshall et al., 2016; Berner et al., 2020). TS values indicate how much each variable is changing per month per year. Based on the TS values, the FCA were categorized in the following categories:

(i) GPP (+) ET (+) WUE(+)

(ii) GPP (+) ET (–) WUE(+)

(iii) GPP (+) ET (–) WUE(–)

(iv) GPP (+) ET (+) WUE(–)

(v) GPP (–) ET (–) WUE(–)

(vi) GPP (–) ET (+) WUE(+)

(vii) GPP (–) ET (+) WUE(–)

(viii) GPP (–) ET (–) WUE(+)

These categories were defined regardless the statistical significance of the GPP, ET and WUE changing rates (+ for increasing rates, – for decreasing rates).

The total month carbon increase or decrease for MODIS pixel was acquired by multiplying the total FCA within the pixel and the TS value of the respective pixel. Then, the total monthly carbon was summed per pixel to identify the FCAs with an annual GPP loss or gain. The FCAs with a GPP gain represent areas where the GPP increase in spring and autumn, for instance, compensated for (offset) the summer GPP decrease. However, if the FCA showed GPP loss, the GPP increase did not offset the GPP decrease.

Finally, the Mann-Kendall (Mann, 1945; Kendall, 1957) test was used to identify the FCAs with significant monthly trend in each one of the variables (GPP, ET and WUE). The significance level used was 95% ($p<0.05$)

# 3. RESULTS

## 3.1. Forest fragmentation in the Brazilian Legal Amazon (Article I)

*Spatio-temporal trends of forest loss*

In **Article I**, the first task was to evaluate the dynamics of the forest loss in the whole BLA to later analyse the forest degradation through fragmentation in the area. Between 2001 and 2017, a total of $36.6 \times 10^6$ ha of forest loss were identified in the BLA (Figure 3). After the rapid increase from 2001 to 2004 (+54%), the forest loss rates showed an overall decrease until 2015 (–48.3). However, in 2016 and 2017 the forest loss rates increased greatly. A similar temporal variation is observed in the trends od the forest loss patches potentially caused by fire. The area of forest loss potentially degraded by fire decreased from $1.3 \times 10^6$ ha (44% of total forest loss) in 2004 to $0.33 \times 10^6$ ha in 2015 (22% of the total forest loss).

During the 2001 to 2017 period, more than $3.8 \times 10^6$ ha of forest loss (10% of the total forest loss in the BLA) occurred within conservation and indigenous reserves (Figure 3). From the total forest loss, the majority (53%) was within sustainable use areas (a specific type of conservation unit), while indigenous reserves and integral protection units shared the remaining forest loss area (36% and 9% respectively). The 2% left occurred within overlapping areas of conservation units and indigenous reserves.

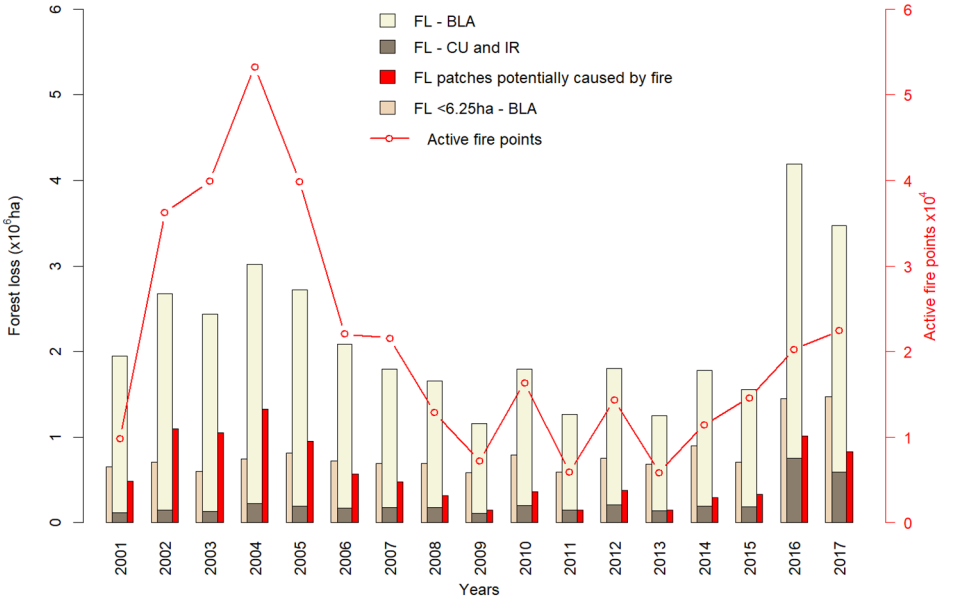


**Figure 3**. Annual forest loss (FL) area within and outside conservation units (CU) and indigenous reserves (IR), as well as the area occupied by forest loss patches smaller than 6.25 ha in the BLA and the number of active fire points within the forest loss patches and the forest loss area potentially caused by fire. Source: **Article I**, Figure 1B.

The spatio-temporal analysis also indicated that the forest loss area of patches <6.25 ha remained the same from 2001 to 2015. However, the proportion of the forest loss from these patches increased during the period as the total annual forest loss area decreased (Figure 3).

Figure 4 shows that from 2001 to 2017, $23.4 \times 10^6$ ha of forest loss took place within primary forest areas (7% of the total area of primary forest in 2000) whereas $13.2 \times 10^6$ ha in non-primary forest areas (17% of the total non-primary forest in 2000). Forest loss decreased significantly in both forest types from 2001 to 2015, but no significant trend is identified when forest loss in 2016 and 2017 were included. The mean size of forest loss patches decreased significantly ($P < 0.05$) in both forest types, mainly due to the decreased number of large forest loss patches (>6.25 ha) since 2004 to 2006.

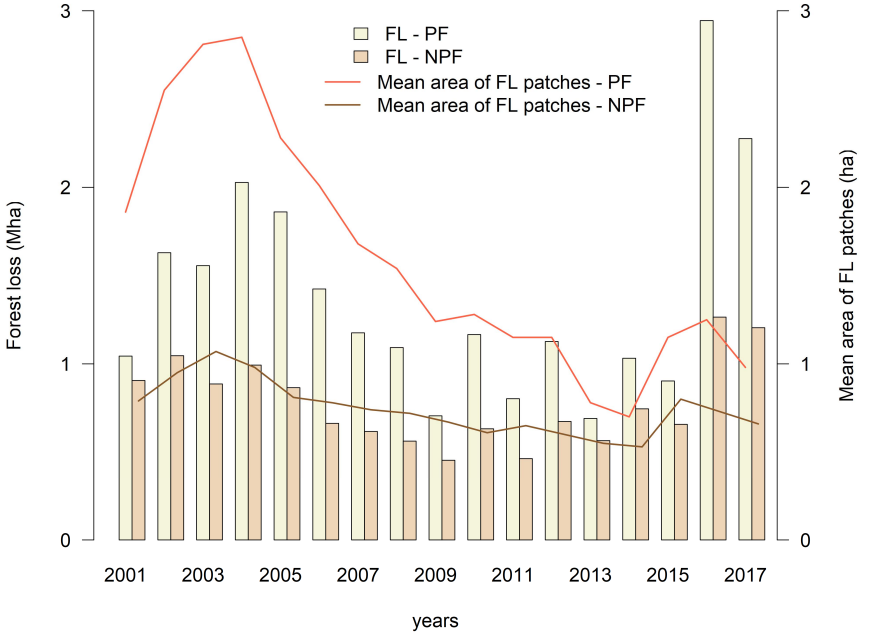


**Figure 4**. Total forest loss (FL) and mean patch size of forest loss patches in primary forest (PF) and non-primary forest (NPF). Source: **Article I**, Figure 3.

Statistically significant trends showed a clear increasing pattern in Amazona, Pará, Acre, and Maranhão states (Figure 5). These states are located outside of the so-called "arc of deforestation", which extends from Maranhão to Rondônia and was the main agriculture frontier during the early 2000s (Fearnside, 2005). From the 51142 grid cells, 20.5% showed increasing trend in forest loss whereas only 10% showed decreasing trend (Figure 5). The decreasing trends cells were mainly located in the former deforestation areas, where most of the forest loss had occurred before the study period.

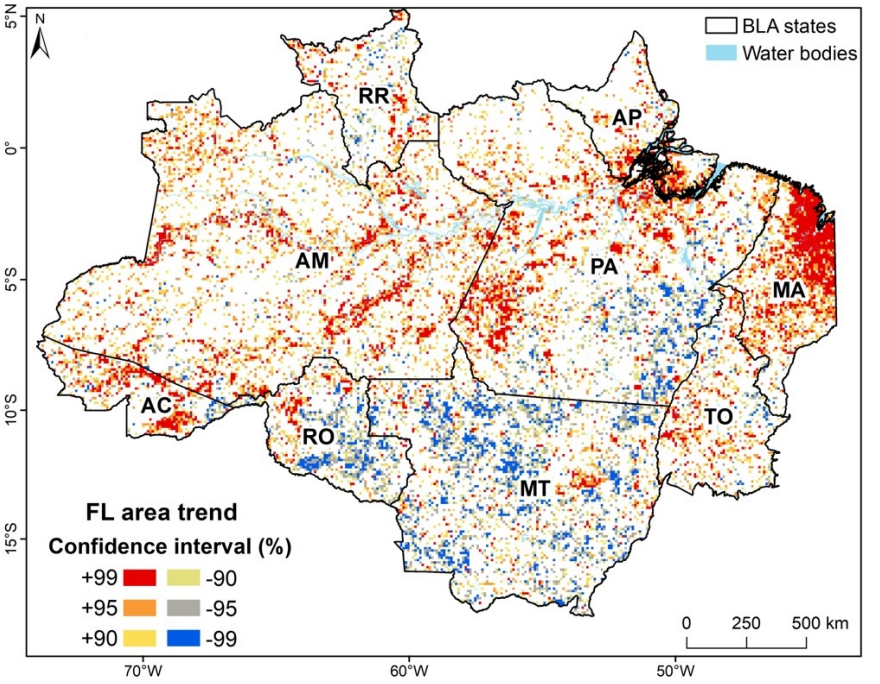


**Figure 5.** Spatial patterns of forest loss areas trends in the Brazilian Legal Amazon (BLA). The confidence levels for the trends were estimated using the Z values. For the confidence intervals (CIs), $z \geq 2.576$ for the 99% CI, $2.576 > z \geq 1.960$ for the 95% CI, and $1.960 > z \geq 1.645$ for the 90% CI. Brazilian states: Acre (AC), Amazonas (AM), Amapá (AP), Maranhão (MA), Mato Grosso (MT), Pará (PA), Roraima (RR), Rondônia (RO), and Tocantins (TO). Source: **Article I**, Figure 5A.

*Forest cover fragmentation*

The forest cover fragmentation analysis revealed that from 2000 to 2017 the number of forest fragments increased 68.5% (from $>5.2 \times 10^6$ fragments to $>8.8 \times 10^6$ fragments). At the same period, the mean patch size of the forest cover fragments decreased from 77.5 to 41.8 ha. Interestingly, the rate of fragmentation (new forest fragments) increased after 2010 despite the decrease in the forest loss rates, with significant rate values in 2016 and 2017. The intensification in the fragmentation rates was more evident in the forest areas outside of conservations units and indigenous reserves (Figure 6A). Within conservation units and indigenous, forest fragments increased from 800 000 in 2000 to 1.2 million fragments in 2017 (Figure 6A).

We also observed that the number of non-primary forest fragments increased 31.5% from 2000 ($6.2 \times 10^6$ fragments) to 2017 ($8.15 \times 10^6$ fragments) while the number of primary forest fragments increased 480% during the same period (from $0.5 \times 10^6$ fragments in 2000 to $2.9 \times 10^6$ in 2017; Figure 6B). Most of the new primary forest fragments were <50 ha as the number of forest patches with this size increased 448% (from $0.5 \times 10^6$ fragments to $2.9 \times 10^6$ fragments).

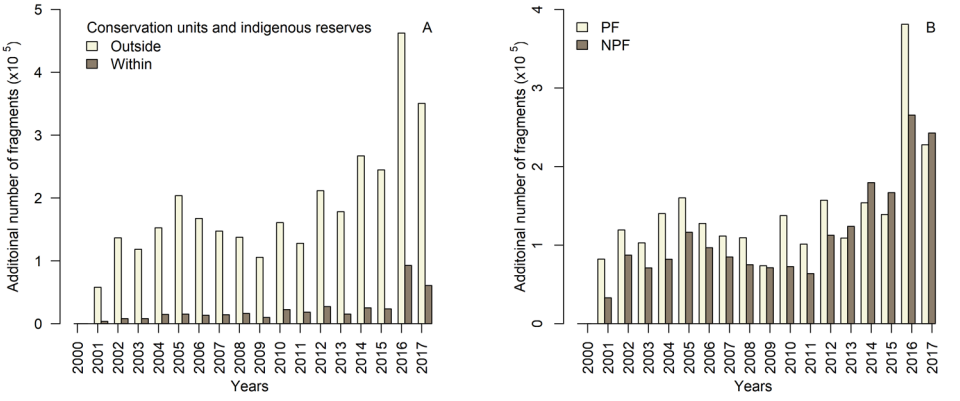


**Figure 6**. Changes in the number of forest cover fragments (A) within and outside conservation units (CU) and indigenous reserves (IR) and (B) for primary forest (PF) and non-primary forest (NPF). Source: **Article I**, Figure 7.

The fragmentation of primary and non-primary forest has resulted in a widespread decrease in the mean forest patch size, as illustrated in Figure 7. Almost half (40.6%) of the grid cells had forest cover patches <50 ha by 2017 (Figure 7A) and 68.7% showed a significant decrease trend in the mean patch size from 2000 to 2017 (Figure 7B).

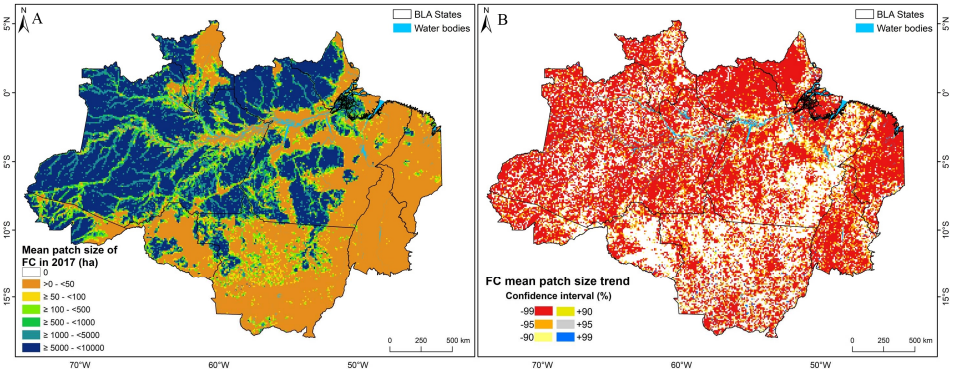


**Figure 7.** Mean patch size of cells with forest cover in 2017, and statistically significant changes (Mann–Kendall test) in the mean forest cover patch size from 2001 to 2017. Source: **Article I**, Figure 8 C and D.

## 3.2. Evapotranspiration shifts over vegetation areas in the Baltic countries (Article II)

*Unchanged forest areas*

In 2000, more than half of the Baltic countries were covered by forest (53.1%). By 2018, the total forest area decreased only by 0.4% as2,532.1 $km^2$ of forest was converted to cropland. However, only 72.8% of the forest area remained completely unchanged throughout the study period.

*Spatio-temporal precipitation analysis*

Monthly precipitation analysis indicated that half of the months showed no significant trend between 2000 and 2018 (Figure 8). April, September and December showed significant increasing trends in 13.6, 3.1, and 8.1% of the total pixels (2557 pixels) whereas March, June, and July presented significant decreasing trends in a small proportion of the pixels (0.8, 1.4, and 0.2% of the total, respectively). The pixels with statistically significant decreasing trend were spatially mainly concentrated in the south-west of Lithuania (in March and June), while the pixels with increasing trend were not only in the south and southwest of Lithuania and Latvia but also in the northeast of Estonia (Figure 8). The rate of the trends revealed by the SS values for significant ($p < 0.05$) and non-significant trends ($p > 0.05$) indicated that September showed an average increase of $2.37 \pm 0.29$ mm per year (mean ± SD) for increasing pixels. That is greater than the increasing rates of April ($1.60 \pm 0.26$ mm per year) and December ($1.31 \pm 0.32$ mm per year). March, June, and July showed similar SS decreasing values (1.66, 2.33, and 2.22 mm per year respectively).

*Spatio-temporal temperature analysis*

Similarly to the precipitation analysis, the monthly mean temperature analysis showed that 8 months showed no significant trends ($p < 0.05$) in any pixel (Figure 9). Additionally, no pixels with statistically significant decreasing trend were observed. Significant increasing trends were identified in May (6.2%), June (4.6%), August (16.6%) and September (89.3%). In September, the pixels with a significant increasing trend covered almost the entire region, while in May, June and August, the pixels were clustered in northern and western Estonia and eastern Latvia and Lithuania (Figure 9). The average TS values of the significant increasing pixels were similar among the months (May = 0.14°C per year, June and August = 0.10 °C per year, September = 0.13 °C per year).

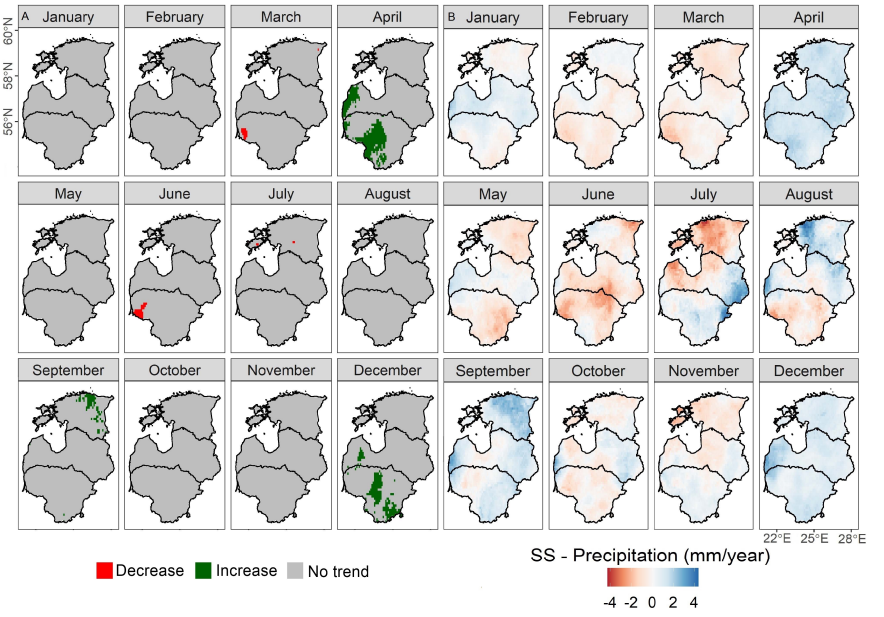


**Figure 8.** (A) The results of the Mann-Kendall test for statistically significant ($p < 0.05$) trends in monthly precipitation at the pixel level from 2000 to 2018. (B) Sen's slope (SS) values for changes in precipitation. Positive values represent increasing and negative values represent decreasing precipitation. Source: **Article II**, Figure 2.

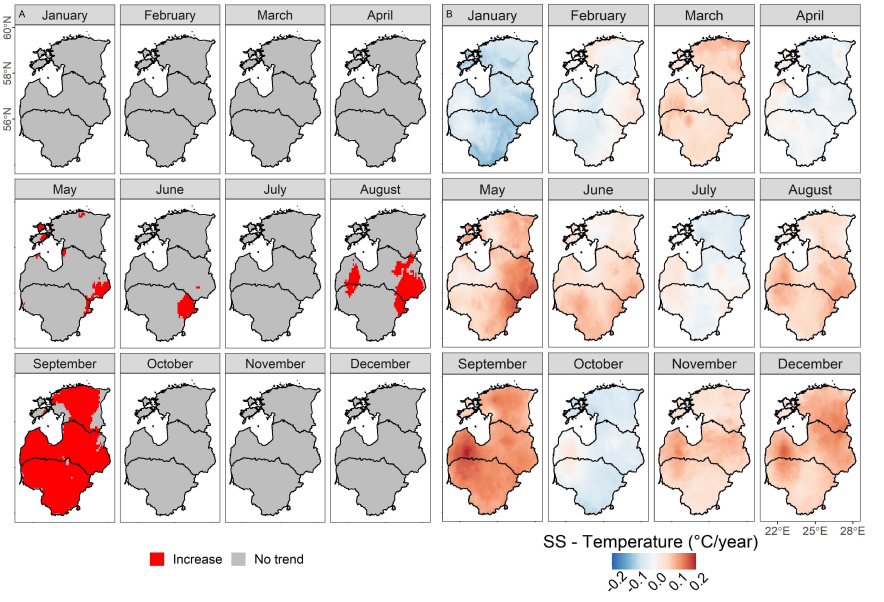


**Figure 9**. (A) Mann-Kendall trend analysis for monthly mean air temperature at a pixel level from 2000 to 2018. (B) Sen's slope values for monthly mean air temperature. Positive values represent a temperature increase, and negative values represent a decrease. Source: **Article II**, Figure 3.

*Spatio-temporal ET analysis from 2000 to 2018*

Pixels with significant ($p < 0.05$) increasing and decreasing trends for ET were spatially scattered over the study region (Figure 10). In May, June, and September, 23.2, 9.1, and 15.2% of the pixels (from a total of from 1 423 312) showed increasing ET trends, with mean TS values of $1.41 \pm 0.50$ (mean ± SD), $1.69 \pm 0.67$, and $0.65 \pm 0.31$ mm per year (Figure 10), respectively. August also showed high percentage of pixels with increasing trend (9.3%), but more concentrated in the eastern part of the region. November, on the other hand, showed the biggest percentage of pixels with a decreasing trend for ET (9.5%). The remaining months (March, April, July, and October) showed <2.5% of the pixels with either increasing or decreasing trend. For these months (except July), the pixels with no significant trend revealed an average increase in the ET rates.

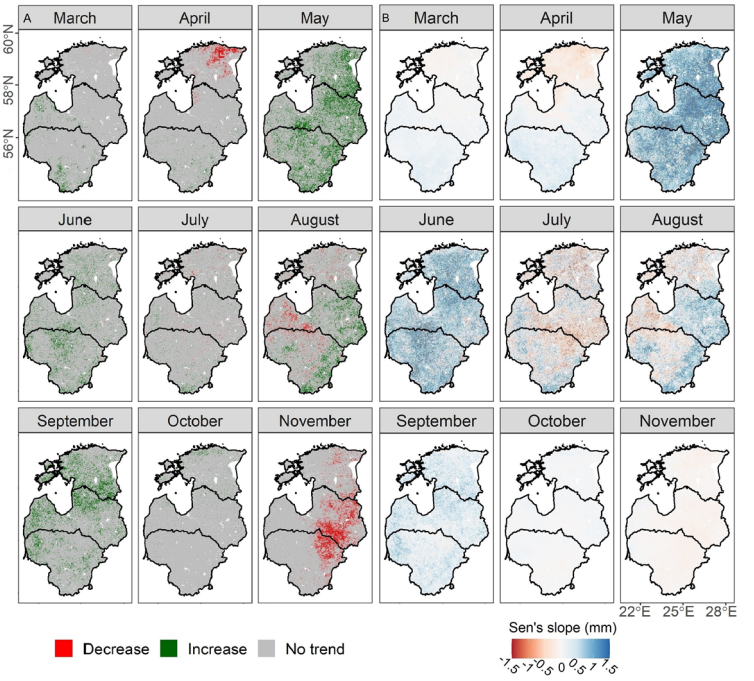


**Figure 10**. (A) Mann-Kendall trend analysis for evapotranspiration at a pixel scale for each month from 2000 to 2018, with $p < 0.05$ for significant trends. (B) Sen's slope values for evapotranspiration in each month. Positive values represent an increase, and negative values a decrease. Source: **Article II**, Figure 4A.

In the seasonal analysis, 13% of the pixels in autumn and 13.5% in spring presented a significant increasing trend, which is more than the proportion in summer (10%) All seasons had approximately 1% of the pixels showing decreasing trend and they were spatially spread spread across the Baltic countries during summer and autumn. The pixels with increasing trend shows spatial spread in all three seasons. On an annual basis, the spatio-temporal analysis revealed that 34.9% of the pixels had a significant increasing trend and only 0.3% showed a significant decreasing trend.

*Spatio-temporal ET analysis of forest pixels from 2000 to 2018*

The analysis indicated that 48.1%of the MODIS ET pixels had forest as the major LULC type (covering >50% of the MODIS ET pixel area). Most of these pixels (>77%) had no significant monthly trend in ET. Less than 6% of the forest showed decreasing trends, with November showing the highest percentage (5.8%) (Figure 11). For March, April, October, and November, less than 2%) of the forest pixels showed increasing trends.

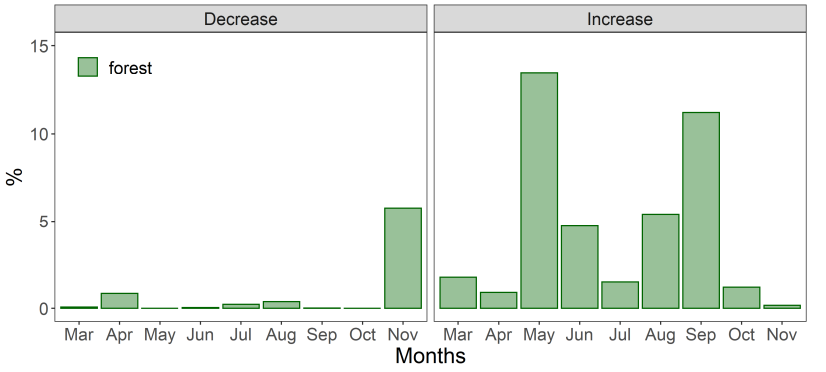


**Figure 11**. Percentage of forest pixels (>50% of the MODIS ET pixel area) that showed decreasing and increasing trends in each month from 2000 to 2018. Source: **Article II**, Figure 4B and C.

*Evapotranspiration over unchanged forest*

Unchanged forest areas were the major LULC type within 10 949 MODIS ET pixels. By using the monthly ET average of these pixels, no significant trend was identified in any of the moths. However, the SS of forest pixels show an ET increase in 6 out of 9 months, with May (0.7 mm per year), June (0.55 mm per year), and September (0.35 mm per year) showing the highest increasing values (Figure 12). September very likely drove the significant increase in autumn (the other seasons did not show significant trends). On the annual analysis, the forest pixels had a statistically significant increasing trend of 3.46 mm per year.

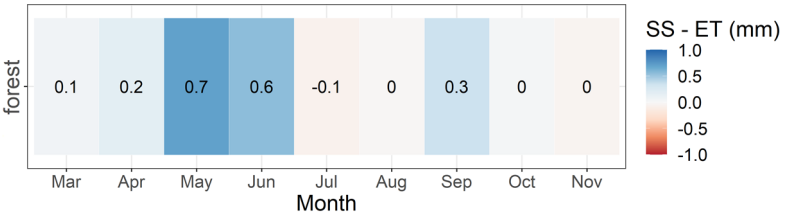


**Figure 12**. Sen's slope (SS) values of evapotranspiration (ET mm) for forest in each month from 2000 to 2018. Source: **Article II**, Figure 5.

## 3.3. Carbon assimilation and efficient water usage over European forest core areas (Article III)

*Unchanged European forest areas*

From 1986 to 2020, approximately 1.8 × 106 km$^2$ of the European forests remained unchanged. However, ~99.6% were located within the 500 meters from the forest edge, which were removed from the analysis. The remaining forest area (hereafter called forest core areas – FCA) was 6468.9 km$^2$ (0.4% of the total unchanged forest area). Countries in eastern Europe (Poland, Croatia, Ukraine, Bosnia and Herzegovina, Belarus, and Romania) contained the largest area of FCA (Figure 13). As we only analysed the the MODIS pixels with >50% of their area covered by FCAs, the final total forest area analysed was 3601.5 km$^2$ (or 0.001% of the total undisturbed forest area in Europe).

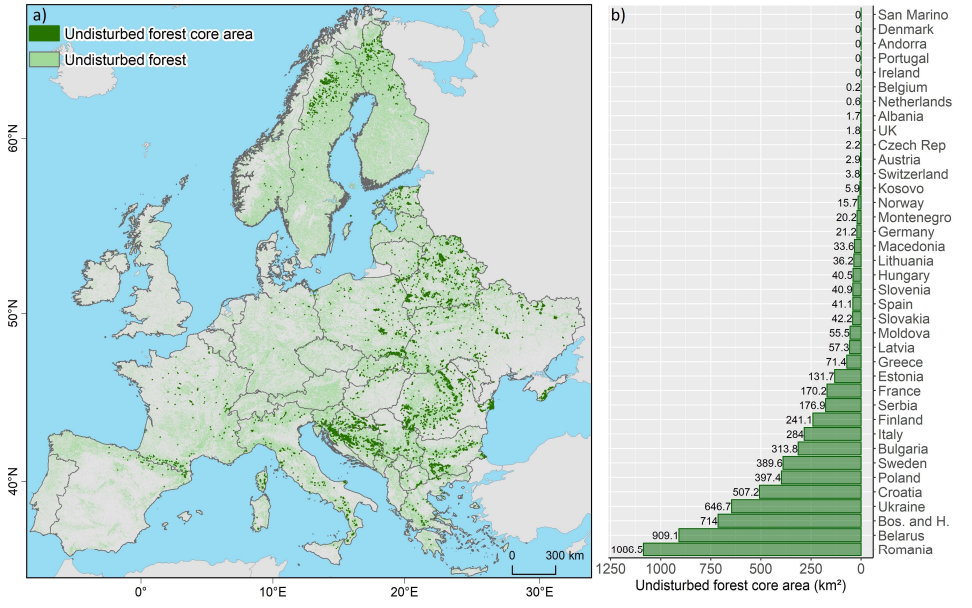


**Figure 13**. A) Spatial distributions of undisturbed forest cover and undisturbed forest core areas in 2020. B) Undisturbed forest core area size by country in 2020. Forest core areas were >500 m from the edge of the undisturbed forest patches Borders of the forest core areas have been exaggerated for visualization. Source: **Article III**, Figure 1.

*Spatio-temporal GPP, ET and WUE trends*

Most FCA showed no significant trend in the monthly GPP (>85%), ET (>76%) and WUE (>62%) between 2000 and 2020. The few FCA that showed significant increasing trend in GPP were spatially scattered throughout eastern, southern, and northern Europe (Figure 14A) and temporally concentrated in early to mid-spring (March 12.1% and April 14.6% from the total FCA of 3601.5 km$^2$) and mid- to

late autumn (October 5.2% and November 12.5%; Figure 14B). The statistically significant decreasing trends were occurring in late spring (May 7.7%), early summer (June 3.8%), and early autumn (September 4.4%), and clustered in the south-eastern part of Europe. Comparing the median TS values for pixels with significant trends revealed that the magnitudes of the decreasing TS values were greater than the magnitudes of the increasing TS values for most months (6 out of 9 months) (Figure 14C). However, it can be observed that the total annual GPP change for FCAs with increasing trends was greater (3.3 Mt C/year) than for FCAs with decreasing trends (2.0 Mt C/year) (Figure 14D). That resulted in a annual net carbon gain of 1.3 Mt C per year.

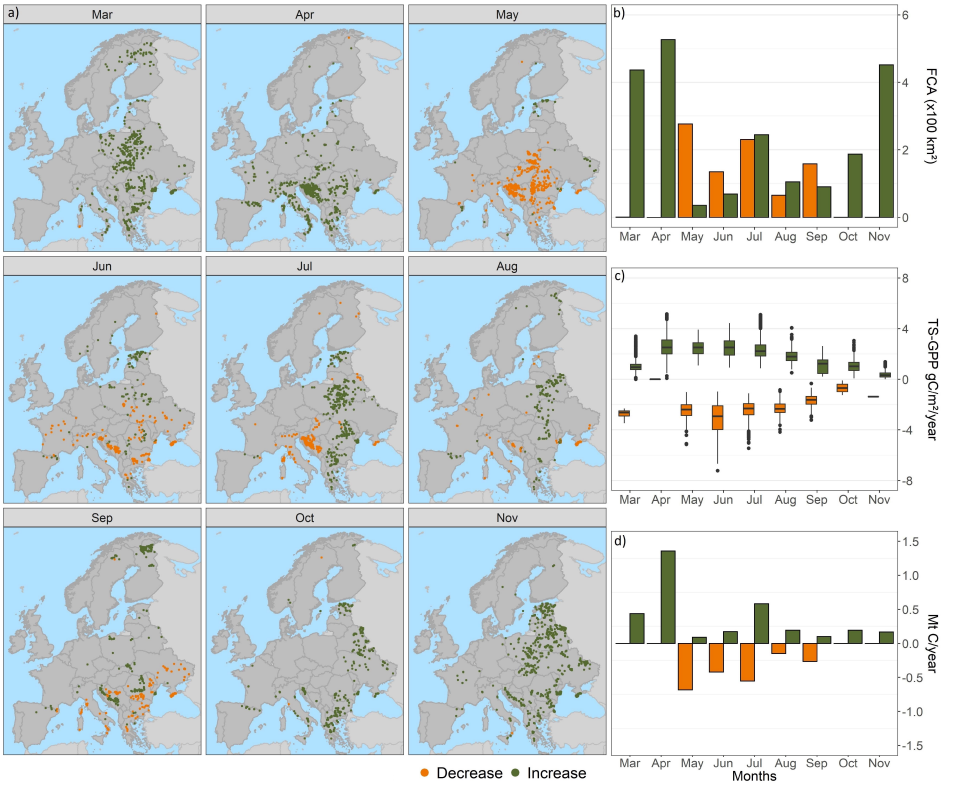


**Figure 14**. A) Statistically significant (95% confidence interval) spatial and temporal trends for monthly gross primary production (GPP) of forest core areas (FCAs) from 2000 to 2020. B) FCA areas that showed significant increases or decreases in GPP. C) Theil– Sen's slope (TS) values for pixels with increasing and decreasing GPP trends at a monthly time step. D) Monthly total carbon change for the increasing and decreasing GPP trends. Significant trends were identified using the Mann-Kendall test for each month. Source: **Article III**, Figure 2.

In contrast with GPP, more FCAs showed significant increasing trends in ET than showed decreasing trends for all the months analyzed (Figure 15). Only May showed more decreasing trends, which were clustered in south-eastern Europe (Figure 15A/B). June, August and September showed the greatest proportion of FCAs with increasing trends that were mainly located in eastern Europe (Figure 15A). The remaining months showed no clear spatial pattern for the ET trends (Figure 15A). Additionally, the TS values of the FCA with increasing ET trends were higher than the FCA with decreasing trends for most months (6 out of 9) (Figure 15C). However, the difference between the TS values of both trends was smaller than the difference of the GPP TS values (ratio was close to 1).

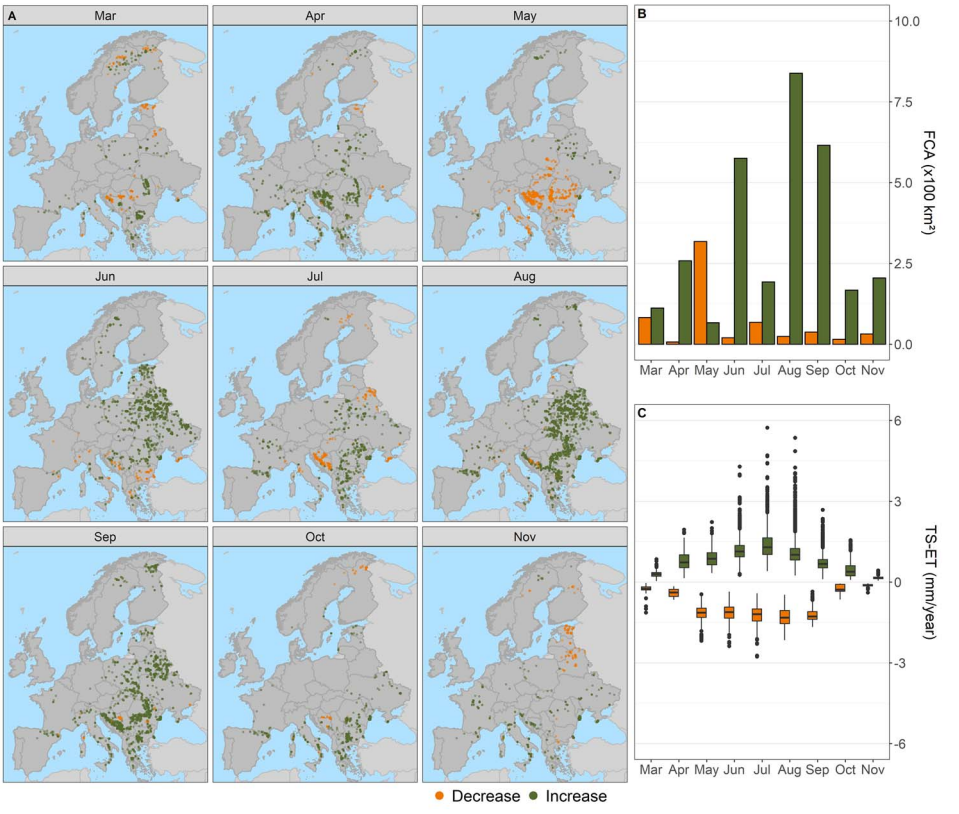


**Figure 15**. A) Distributions of forest core areas (FCAs) with statistically significant ($p < 0.05$) increasing or decreasing trends for monthly evapotranspiration (ET) from 2000 to 2020. B) Total FCA area that showed a significant increase or decrease in ET. C) Theil–Sen's slope (TS) values for the increasing and decreasing ET trends at a monthly time scale. Significant trends were identified using the Mann-Kendal test for each month. Source: **Article III**, Figure 3.

The WUE analysis indicated that the FCA with significant decreasing trends were spread throughout Europe, especially during the summer and early autumn, whereas FCA with significant increasing trends were mainly clustered in eastern Europe during the spring and late autumn (Figure 16A). In terms of the area of FCAs (Figure 16B), the area with increasing WUE was greater than the area with decreasing WUE in 5 months (May to September). Interestingly, the median TS values for FCAs with increasing trends in early spring and late autumn were at least 1.5 times greater than the TS values of FCAs with increasing trends in the remaining months (Figure 16C). Additionally, the TS of FCAs with a significant increase of WUE had a greater magnitude than in areas with a significant decrease in four of the nine months (Figure 18C).

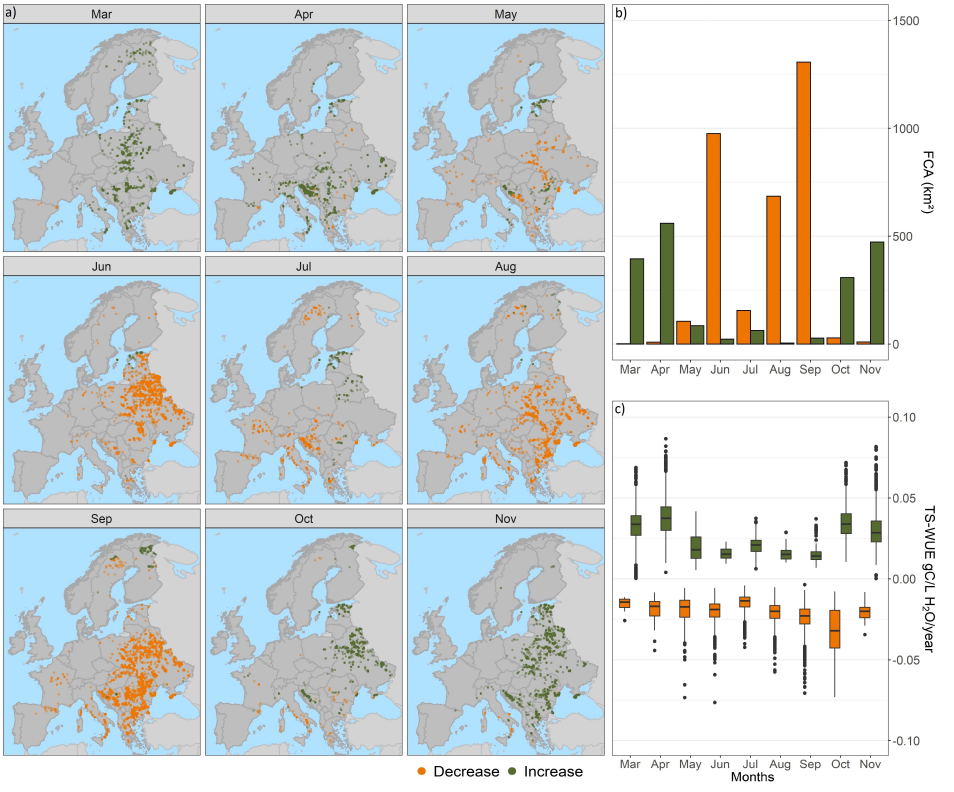


**Figure 16**. A) Distributions of forest core areas (FCAs) with statistically significant ($p<0.05$) increasing or decreasing trends for monthly-scale water-use efficiency (WUE) from 2000 to 2020. B) Total area of FCAs with significant increases or decreases in WUE. C) Theil–Sen's slope (TS) values for increasing and decreasing WUE trends at monthly time scale. Significant trends were identified using the Mann-Kendal test for each month. Source: **Article III**, Figure 4.

*Interaction between GPP, ET and WUE trends*

By combining the negative and positive TS values of GPP, ET and WUE, regardless of their statistical significance, we found that almost half of the FCA had a concomitant increase in GPP, ET and WUE during early spring and late autumn (Figure 17). That indicates that the WUE increase in these periods was not due to a decrease in ET, but rather because of a greater GPP increase compared with the ET increase. During summer, on the other hand, more FCA showed increasing GPP together with decreasing WUE. Additionally, most FCA showed decrease in GPP and WUE during summer due to the ET increase (Figure 17).

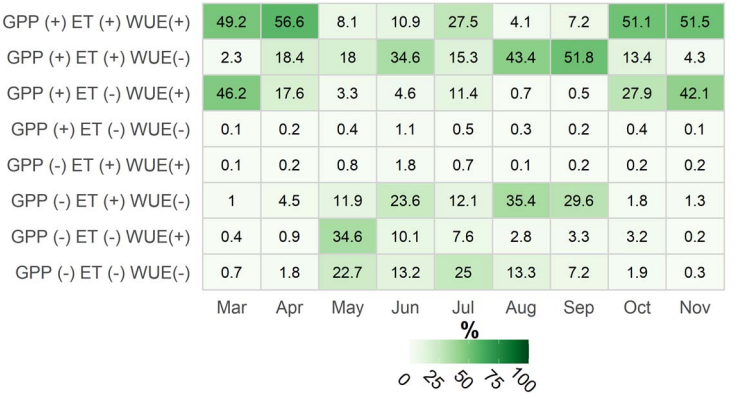


**Figure 17**. Proportions (%) of the total forest core areas (FCA) that showed an increase (+) or decrease (–) in gross primary production (GPP), evapotranspiration (ET), and water-use efficiency (WUE). Source: **Article III**, Figure 5.

*GPP compensation*

More than 93% of the FCA showed either GPP decrease or increase (significant or not) in at least one of the months analysed. Although November showed the largest area of FCAs with GPP increase (98%), April was the month with the greatest positive GPP (5 Mt/year; Figure 18A) balance (total increase minus total decrease within the month). May showed the largest area of FCAs with decreasing GPP (70%) and with negative GPP balance (–2.3 Mt/year; Figure 18A). By multiplying the monthly TS values for GPP by the FCAs in each pixel, we identified that 75.1% of the FCAs showed an annual net gain in GPP (increase minus decrease) of 9538.7 t C per year (Figure 18B). For the remaining 24.9% of the FCAs that showed decreased GPP, the total net loss was 1960.8 t C per year (Figure 18B). Therefore, the net carbon balance for GPP in the FCAs totalized a net gain of 7577.9 t C per year. The FCAs with net loss in GPP were clustered in northern and southern Europe (Figure 18C), whereas FCAs with net gain in GPP were scattered throughout Europe (Figure 18D).

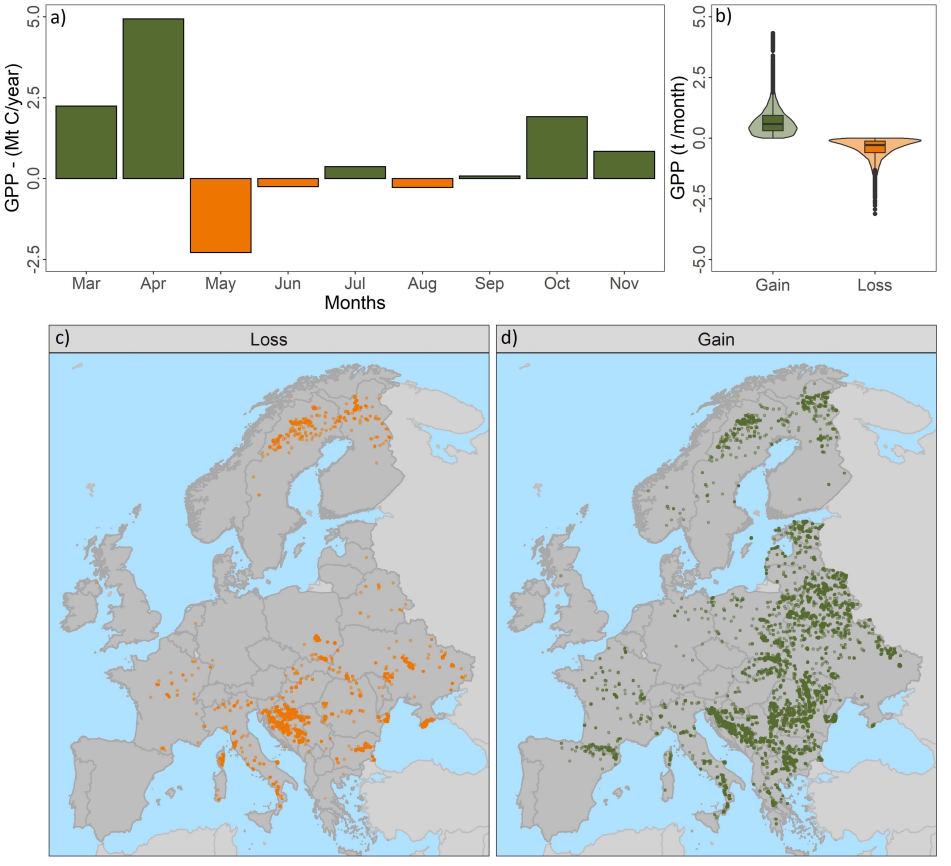


**Figure 18**. A) Gross primary production (GPP) compensation (total increase minus total decrease) for forest core areas (FCAs) at a monthly time step. B) Boxplots of the annual net GPP gain and loss for all FCAs across Europe, where the black horizontal lines are the medians and the shaded area is the frequency of the values. C) Spatial distribution of FCAs with annual net GPP loss. D) Spatial distribution of FCAs with annual net GPP gain. Source: **Article III**, Figure 6.

# 4. DISCUSSION

The case studies in this dissertation provided insights into the direct and indirect human-induced forest degradation in regions with different climates. **Article I** (discussed in section 4.1) revealed the direct human-induced forest degradation caused by forest fragmentation and its relationship with the spatial and temporal dynamics of forest loss. **Articles II** and **III** (discussed in sections 4.2 and 4.3) revealed the effects of the indirect human-induced forest degradation and the associated reduction in the provision of forest ecosystem services (water cycling and carbon assimilation) due to anthropogenic climate variability and long-term climate change.

## 4.1. Direct human-induced forest degradation by forest fragmentation

Forest loss, which also includes areas of degraded forest created by fire or selective logging, decreased significantly from 2004 to 2012 in Brazilian Amazon, as has been reported by previous studies (Richards et al., 2016). This reduction has mainly resulted from a decrease in the number of the large forest loss patches (Rosa et al., 2012) that were the target of the PPCDAm (Nepstad et al., 2014) and the Soy Moratorium (Gibbs et al., 2015). Therefore, both initiatives have played an important role in reducing forest loss rates and, as a result, in reducing forest degradation. However, the number of small forest loss patches (<6.25 ha) increased throughout the study period, indicating that direct human-induced forest degradation continues on a smaller scale. The increase in the number of small forest loss patches may be related to a strategy adopted by the landlords to avoid the government's deforestation monitoring systems (Rosa et al., 2012; Schneider and Peres, 2015; Richards et al., 2016). Moreover, **Article I** reinforced this possibility because the study showed that the forest loss patches not only became smaller but also spread out more, indicating that dispersion may have been an additional strategy to escape the monitoring system.

Although the forest loss rates decreased after 2004, the forest areas vulnerable to degradation did not decrease because the number of new forest fragments showed an increasing trend due to the increased number of small forest loss patches. These results confirm the findings of simulations that also suggest forest fragmentation increases despite a decreased forest loss (Taubert et al., 2018). This upward trend in the fragmentation and the reduction of the sizes of forest patches can potentially increase the forest degradation, as more areas will become susceptible to fire (Cochrane, 2003) and edge effects (Keller et al., 2008). The edge effects, for instance, were responsible for the loss of 947 Tg of carbon due to degradation of the forest biomass within the edges of the Amazon forest from 2001 to 2015 (Silva et al., 2020). This carbon loss corresponds to one-third of the losses from deforestation. In addition, the shift of forest fragmentation to areas in

the inner BLA with high net primary production (Malhi et al., 2009; Aragão et al., 2010) will not only increase carbon emission but also increase forest degradation due to the biomass loss induced by the forest edges (Chaplin-Kramer et al., 2015). Therefore, the spatial shifts in the forest loss dynamics are driving the forest degradation to areas in the BLA that were formerly considered intact (Potapov et al., 2017).

The spatial shifts of the areas of forest loss have also modified the process of forest degradation through fragmentation between primary and non-primary forests. Before 2013, both forest types showed a similar pattern in forest cover fragmentation. However, after 2013 the forest fragmentation became more intense in non-primary forest areas, which are not the target of the anti-deforestation initiatives (i.e., PPCDAm and Soy Moratorium). The degradation of the non-primary forest through fragmentation can reduce its potential to act as a large carbon sink that mitigates climate change (Heinrich et al., 2017). Moreover, few conservation units and indigenous reserves are located in the non-primary forest areas, and this makes most of these areas more vulnerable to forest fragmentation. Within conservation units and indigenous reserves, the forest cover fragmentation was less intense than outside of these areas. That demonstrates the importance of the conservation units and indigenous reserves to improve forest conservation and to reduce or prevent forest fragmentation and degradation in the BLA (Cabral et al., 2018).

Fire occurrence, which is an important driver of forest degradation, may also have contributed to the increased number of small forest loss patches. In the BLA, fire occurrence is often related to the deforestation process and to agricultural and pasture management (Lima et al., 2012). However, during drought years, the fire may escape their control and spread into neighbouring forest areas to become a forest fire. This is shown by the increased forest loss in 2016 and 2017, when 24.0 and 23.9% of the patches, respectively, had fire occurrence. This was especially true in 2016, when an intense drought occurred in the BLA (Jiménez-Muñoz et al., 2016; Yang et al., 2018). Intense drought in the Amazon can result from changes in the precipitation regime (Marengo, 2004; Cox et al., 2008) that are triggered by anomalies in sea surface temperatures. During these drought periods, the forest is more susceptible to fire (Aragão et al., 2018), which can increase the area of degraded forest.

## 4.2. Indirect human-induced forest degradation by changes in evapotranspiration and carbon cycles

In my analyses of only the unchanged forest areas, **Articles II** and **III** indicated periods when the provision of forest ecosystem services changed, likely driven by shifts in the climate. These climate-induced alterations in the forested areas (especially reductions of carbon assimilation) can be characterized as indirect human-induced forest degradation since the integrity and maintenance of the ecosystem services related to water and carbon cycles have been compromised (IPCC, 2019).

In general, **Article II** and **Article III** revealed that ET has intensified in the unchanged forested areas in most months and that this effect was widely distributed. During the spring and autumn, the ET intensification can be related to the lengthening of the growing season. Longer growing seasons in temperate regions have been identified in several previous studies, which indicated that increasing temperature and precipitation were the main drivers of ET intensification (Dragoni and Rahman, 2012; Gaertner et al., 2019). Although the ET intensification appears to not be a negative change, degradation of the forest's capacity to control water recycling has a direct impact on the regional precipitation regime and water balance (Cheng et al., 2017; Guo et al., 2017). For example, most of the months with a significant increase in ET and temperature (e.g., March and May; **Article II**) also showed a reduction in the river discharge (Kriauciuniene et al., 2012). The increased ET can also result in a lower soil water availability during the summer (Lian et al., 2020), and when this is combined with decreased precipitation, it can explain the ET reduction during July and August (**Article II**). Moreover, the ET changes in one region can alter the precipitation regimes in other regions (Makarieva et al., 2013; Staal et al., 2018). The analysis of **Article II** supports the hypothesis that the increase of the forest ET was more likely driven by changes in climate variables than by LULC change, as was reported previously (Li et al., 2017). These results suggest that the Baltic region is experiencing a warming trend in most months, in all seasons, and for the whole year, accompanied by a reduction in precipitation in autumn and summer months. The analyses of **Articles II** and **III** also revealed that areas with increasing ET are, in general, widespread, whereas areas with decreasing ET are clustered in certain areas of the Baltic countries (**Article II**) or Europe (**Article III**).

As in the case of **Article II**, analysis of the results of **Article III** indicated that the longer growing season induced a spatially scattered increase of GPP over undisturbed European FCAs in the early spring and late autumn. The GPP increase, especially during the spring, has been linked to a heating-induced change in the phenology of temperate forests and to increases in the atmospheric $CO_2$ concentration (Keenan et al., 2014; Sippel et al., 2017). Under high concentrations of atmospheric $CO_2$, the forest vegetation can photosynthesize more while decreasing the stomatal aperture to reduce the loss of water vapour by transpiration (Guerrieri et al., 2020). This combination of processes led to a concomitant increase of GPP and WUE (i.e., more carbon is being assimilated per unit of water) during early spring and late autumn, despite the increase in ET (i.e., WUE=GPP/ET). Although the combined GPP and WUE increases within most of the FCAs may not be seen as forest degradation, it is important to note that this increased efficiency is not the result of a decrease in ET. In fact, most of the FCAs showed an increase in ET during the early spring and late autumn, as previously discussed. To maintain the spring GPP increase, the vegetation removes water from the soil, which is not replaced due to the reduced spring precipitation that has been observed (Ionita et al., 2020). Therefore, the decreased summer soil moisture (Lian et al., 2020), combined with more frequent droughts (Trenberth et al., 2014), will constrain any potential future GPP increase during the summer.

During the summer, GPP showed a decreasing trend in the FCAs in south-eastern Europe. This degradation of the forest's capacity to assimilate carbon during the summer is related to changes in climate extremes, such as droughts and heatwaves (Keenan et al., 2014; Sippel et al., 2017). Considering that the same FCA can show both trends (increasing and decreasing) at different times, I found that 25% of these areas showed an annual GPP loss. This means that about 900 $km^2$ of FCA have decreased (due to climate change) because the GPP gains did not compensate for the GPP losses. Worryingly, these potentially degraded FCAs with an annual GPP loss are spread across Europe and across different forest types (Copernicus Land Monitoring Service, 2018). Thus, the definition and application of forest management techniques that can enhance carbon assimilation, such as shelterwood cutting and thinning (Lindroth et al., 2018; Puhlick et al., 2020), will be challenging due to the diversity of forest environments. In addition, the total GPP losses in these potentially degraded FCAs were responsible for offsetting 20% of the total GPP increase across the continent. This high proportion demonstrates how carbon losses from degraded forest areas must be considered in national (or global) greenhouse gas estimates (Matricardi et al., 2020; Qin et al., 2021). Moreover, this proportion could increase in the future, as some studies have indicated that in the next 20 to 30 years, ecosystems—including forests—may reach a productivity tipping point (Sperlich et al., 2020; Duffy et al., 2021). At that point, the FCAs may show a productivity reduction that would further exacerbate the reduction of GPP compensation, thereby increasing the area of degraded forests. All these observations have led researchers to question the potential or capability of certain unchanged FCAs to act as nature-based solutions for the mitigation of climate change (Anderegg et al., 2020b).

## 4.3. Limitations and future prospects

It is important to note that the data and methods in all three case studies have some limitations. For instance, the forest loss data (**Article I**) does not include only human-induced forest degradation (e.g., deforestation, selective logging, fire), but also includes natural forest disturbance such as windthrow and natural tree mortality (Harris et al., 2017). Therefore, the annual forest loss rates must be considered cautiously, especially during years with intense drought (e.g., 2010 and 2016). Another limitation is the coarse resolution of the MODIS data used in the three case studies. The MODIS fire data used in **Article I** is provided at a 1-$km^2$ resolution. This means that a fire could begin or be located in any area within the 1-km MODIS pixel. Therefore, the fire maybe not be directly responsible for the forest loss if it is used as a management tool to burn the residual vegetation that remains or that begins to grow after deforestation. The MODIS-based ET and GPP data were validated using ground-based eddy covariance data, but the coarse spatial resolution of the data still limits accurate estimation and can miss variations in the forest composition at the subpixel level that would affect the ET and GPP estimates. However, despite these limitations, the results presented

in this thesis provide objective estimates of the true values and important insights into the direct and indirect human-induced forest degradation.

In future analysis of forest degradation through fragmentation in the BLA, it would be useful to include forest regrowth data and identify the role of regrowth in mitigating forest degradation processes. Moreover, it would be useful to combine data on the driving forces behind the fragmentation to identify the specific causes (e.g., selective logging, small-scale farmers) of fragmentation in different areas of the BLA so that targeted solutions can be developed. To improve the analysis of forest degradation through changes in water and carbon cycles, I recommend stratification of the analysis by forest types using recently developed high-resolution forest type maps (Parente et al., 2021). By using this type of data, improved estimates of GPP and ET could be developed specifically for each forest type. In addition, the new GPP and ET estimates could be done using data-driven models (e.g., machine learning models) or process-based models that use environmental covariates (e.g., atmospheric relative humidity) at higher spatial resolution. This would support the analysis of GPP and ET dynamics at forest edges, as most of the world's remaining forest areas are within 1 km from the edge of the forest (Haddad et al., 2015; Ordway and Asner, 2020).

# CONCLUSIONS

In this thesis, I evaluated the direct and indirect causes of forest degradation using three case studies. The first case study described direct human-induced forest degradation through forest fragmentation in the Brazilian Amazon region. The other two case studies focused on indirect human-induced forest degradation through changes in water and carbon cycles caused by climate change. These case studies describe the condition, health, and quality of the unchanged forest cover in different biomes and under different climate conditions. Therefore, the conclusions in this section provide insights into the necessity of improving measures to combat deforestation and forest degradation and to account for how indirect human-induced forest degradation can hinder the capacity of forest areas to act as nature-based solutions for climate change mitigation.

- Although the anti-deforestation initiatives have played an important role in reducing deforestation in tropical forest across the BLA, they have induced changes in the forest loss process. The decrease in the area of forest loss patches and the spatial shift to new front lines for deforestation in the BLA increased fragmentation of previously isolated areas. That resulted in an increase in forest degradation through fragmentation. Hence, more forest areas are potentially being degraded as a result of the edge effects (e.g., tree mortality) caused by the fragmentation (**Article I**).
- Climate shifts may have degraded the capacity of the forest areas to control their ET. The changes (increases and decreases) in ET rates in undisturbed forest areas occurred at different spatial scales (regional and continental). In the Baltic region, the longer growing season induced an increase in ET during the spring and autumn, versus a decrease during the summer. In contrast, on a continental scale, ET increased during the spring, autumn, and summer in most of the analysed FCAs. These changes in the ET rates influenced the hydrologic cycle differently at different spatial scales (**Article II** and **Article III**).
- The degradation of forest ecosystem services due to changes in the climate prevented some FCAs from acting as carbon sinks. One quarter of the European FCAs showed no GPP compensation across seasons; that is, the GPP increases in spring and autumn could not compensate for the summer GPP decrease. Moreover, the total GPP decrease in the FCAs was responsible for offsetting 20% of the total GPP increase in Europe. Nearly half of the FCAs showed a simultaneous increase in GPP and WUE in the spring and autumn. However, the WUE increase did not result from decreased ET, but rather was due to a GPP increase that was greater than the ET increase. That contradicted the results of some previous studies. These GPP and WUE insights are critically important for assessing the capabilities and limitations of undisturbed FCAs to provide a nature-based solution (e.g., carbon sinks, water pumps) to mitigate global heating (**Article III**).

# ACKNOWLEDGMENTS

I would like to thank my supervisors, Dr Evelyn Uuemaa and Prof Ülo Mander, for all the support, patience and guidance during my journey as a PhD student.

I thank my friends and colleagues, Isaac, Holger, Oleksandr, Iuliia, Desalew, Daniel and Alex for all the help and friendship.

I also thank Dr Michael Marshall for the cooperation and support during my time abroad at ITC Faculty Geo-Information Science and Earth Observation.

Many thanks to my family for keeping me close despite the distance.

# SUMMARY IN ESTONIAN

## Inimmõjust põhjustatud metsade degradeerumise hindamine erinevates bioomides kasutades satelliitandmete ruumianalüüsi

Maailma metsad on tugeva inimmõju surve all. Kui levinuim ja arvestatavaim inimmõju metsadele on raadamine, siis vähem olulised ei ole ka allesjäänud metsade killustumine ja muutused metsade poolt pakutavates ökosüsteemi teenustes (nt. süsiniku- ja veeringe reguleerimine), mis on tihtilugu tingitud inimtekkelisest globaalsest kliimamuutusest.

Metsaökosüsteemid võivad siduda kuni 12% inimtekkelisest süsihappegaasist ning tagastada atmosfääri kuni 40% kohalikest sademetest. Seetõttu on metsaökosüsteemidel oluline roll süsihappegaasi emissioonide vähendamisel ja veeringe reguleerimisel. Metsade degradeerumine võib vähendada fotosünteesi läbi süsiniku sidumist. Fotosünteesi käigus taimed seovad atmosfäärist süsihappegaasi biomassiks samal ajal kui juured võtavad mullast vett, millest osa läheb evapotranspiratsiooni käigus veeauruna atmosfääri. Ökosüsteemi poolt seotud süsihappegaasi kogus väljendub primaarproduktsioonina. Evapotranspiratsiooni ja primaarproduktsiooni dünaamika sõltub keskkonnatingimustest, millest olulisim on kliima. Soojemad temperatuurid kevadel ja sügisel tagavad pikema taimekasvuperioodi, mis omakorda viib suurema primaarproduktsioonini ja seeläbi ka süsiniku sidumiseni. Samas soojemad suved põhjustavad suuremat taimede hingamist, mille käigus süsihappegaas satub tagasi atmosfääri. Seetõttu ei pruugi kevadine ja sügisene suurem süsiniku sidumine olla tasakaalus suvise suurenenud süsiniku emissiooniga metsadest. Lisaks põhjustavad suvised suurenenud temperatuurid suuremat aurumist, mis võib viia vähenenud mullaniiskusele, mis võib paljudes piirkondades saada taimekasvu limiteerivaks teguriks.

Varasemad teadustööd on kasutanud erinevatel ruumi- ja ajaskaaladel kaugseire andmeid metsade muutuste ja degradeerumise hindamiseks. Kuigi tänapäeval on kaugseire andmete kättesaadavus ja kvaliteet oluliselt paranenud, ei ole kahjuks siiani metsaökosüsteemides toimuvate pikaajaliste muutuste uurimiseks piisavalt kõrge lahutusega ja ühtlase ning pika kaugseire andmete aegread kättesaadavad või isegi puuduvad. Seetõttu on metsade degradeerumisest tulenevate süsinikuemissioonide hinnangud sageli puudulikud ning neid ei arvestata riiklikes aruannetes. Samas võivad mõnede hinnangute kohaselt need emissioonid ulatuda neljandikuni kogu metsatustumisest tulenevast süsinikuemissioonist. Veelgi enam – püsiva metsade degradeerumise seire puudumine piirab oluliselt võimekust hinnata metsade suutlikkust toimida looduspõhise lahendusena (Nature-based Solutions NBS) kliimamuutuste leevendamisel.

Käesoleva doktoritöö eesmärgiks oli hinnata kahte metsade degradeerumisega seotud protsessi: (1) troopilise vihmametsa killustumist ja (2) muutuseid evapotranspiratsioonis ja süsinikuringes häiringuteta metsades. Metsade killustumist käsitleti otsese inimmõju tagajärjena, kuna see on peamiselt põhjustatud metsade raadamisest ehk metsatustumises. Seevastu muutuseid evapotranspiratsioonis ja süsinikuringes käsitleti kui kaudse inimmõju tulemust, kuna need protsessid on

peamiselt tingitud inimtekkelisest globaalsest kliimamuutusest. Eelpool mainitud metsade degradeerumise hindamiseks kasutati satelliitandmeid ja ruumianalüüsi kolmes erinevas juhtumiuuringus. Esimeses uuringus analüüsiti satelliitandmestike põhiste metsade muutuste kaartide alusel metsade killustumist Brasiilia Amasoonias aastatel 2001 kuni 2017. Kahes ülejäänud uuringus vaadeldi muutusi vee- ja süsinikuringes Baltikumi ja Euroopa metsades. Nendes uuringutes keskenduti häiringuteta metsade tuumaladele, mis jäid serva mõjualast välja. Uurides muutumatuna püsinud metsamassiive, on võimalik tuvastata kliimamuutuse mõju metsaökosüsteemi vee- ja süsinikuringele. Seejuures on oluline vaadelda vee- ja süsinikuringlust mitte ainult aastate kaupa, vaid ka kuude kaupa, tuvastamaks võimalikke sesoonseid muutusi.

Käesoleva doktoritöö tulemused näitasid, et kuigi Brasiilias on metsatustumise vastased poliitikad vähendanud metsade raadamist, siis samal ajal on suurenenud metsade killustumine, sest raiutakse väiksemate eraldiste kaupa ja liikudes endiselt varem raadamata metsamassiivide sisse (Artikkel I). Seetõttu väheneb aja jooksul Brasiilia Amasoonias järelejäänud metsafragmentide keskmine suurus. Koos kasvava metsa killustumisega kahandab see elurikkust ja soodustab kasvuhoonegaaside emissioone ning süsinikukadusid. Killustunud metsas on rohkem metsaserva, kust süsinikukaod on suuremad nii leostumise kui ka gaasilise emissioonina.

Baltikumi ja Euroopa muutumatuna püsinud metsamassiivide (tuumalade) analüüs (Artiklid II ja III) tuvastas viimase 20 aasta jooksul perioodid, mil evapotranspiratsioonis esinesid muutused, mis on suure tõenäosusega tingitud kliimamuutustest. Evapotranspiratsiooni suurenemine ja vähenemine esines nii regionaalsel (Baltikumi) kui ka kontinentaalsel (Euroopa) tasandil. Baltikumis leiti, et pikem taimekasvuperiood on suurendanud evapotranspiratsiooni kevadel ja sügisel, kuid samal ajal on suvel evapotranspiratsioon mõnedes piirkondades vähenenud. Seevastu Euroopa tasandil suurenes enamikus metsade tuumaladest evapotranspiratsioon kõigil kolmel aastaajal (kevadel, suvel ja sügisel). Kuigi evapotranspiratsiooni suurenemisel ei ole metsade ökosüsteemile otseselt negatiivset mõju, siis võib sellel olla ebasoovitav mõju regiooni veeringele, sest suurenenud evapotranspiratsioon suurendab tõenäosust, et suveperioodil on mullas vähem vett, mis omakorda suurendab põuaohtu.

Töö tulemustest selgus, et neljandikus Euroopa metsade tuumalades ei suuda kevadel ja sügisel suurenenud primaarproduktsioon kompenseerida suvist primaarproduktsiooni vähenemist ning aastane summaarne primaarproduktsioon on kokkuvõttes vähenenud ja süsinikku seotakse vähem. Vähenenud primaarproduktsiooniga metsamassiivid paiknesid üle kogu Euroopa ning hõlmasid erinevaid metsatüüpe, mis teeb keeruliseks anda väga üheseid metsamajanduslikke soovitusi süsiniku sidumise parandamiseks. Kliimamuutuste mõjul võib metsade primaarproduktsioon väheneda veelgi rohkem, mis seab kahtluse alla varasemalt eeldatud metsade võimekuse leevendada kliimamuutuste mõjusid.

# REFERENCES


Abram, N. J., Abram, N. J., Henley, B. J., Gupta, A. Sen, Lippmann, T. J. R., Clarke, H., et al. (2021). Connections of climate change and variability to large and extreme forest fires in southeast Australia. *Commun. Earth Environ.* 2. doi:10.1038/s43247-020-00065-8.

Alencar, A. A., Brando, P. M., Asner, G. P., and Putz, F. E. (2015). Landscape fragmentation, severe drought, and the new Amazon forest fire regime. *Ecol. Appl.* 25, 1493–1505. doi:10.1890/14-1528.1.

Alkama, R., and Cescatti, A. (2016). Biophysical climate impacts of recent changes in global forest cover. *Science (80–. ).* 351, 600–604. doi:10.1126/science.aac8083.

Anderegg, W. R. L., Trugman, A. T., Badgley, G., Anderson, C. M., Bartuska, A., Ciais, P., et al. (2020a). Climate-driven risks to the climate mitigation potential of forests. *Science (80–. ).* 368. doi:10.1126/science.aaz7005.

Anderegg, W. R. L., Trugman, A. T., Badgley, G., Anderson, C. M., Bartuska, A., Ciais, P., et al. (2020b). Climate-driven risks to the climate mitigation potential of forests. *Science (80–. ).* 368. doi:10.1126/science.aaz7005.

Anderson, L. O., Ribeiro Neto, G., Cunha, A. P., Fonseca, M. G., Mendes de Moura, Y., Dalagnol, R., et al. (2018). Vulnerability of Amazonian forests to repeated droughts. *Philos. Trans. R. Soc. B Biol. Sci.* 373, 20170411. doi:10.1098/rstb.2017.0411.

Aragão, L. E. O. C. (2012). The rainforest's water pump. *Nature* 489, 217–218. doi:10.1038/nature11485.

Aragão, L. E. O. C., Anderson, L. O., Fonseca, M. G., Rosan, T. M., Vedovato, L. B., Wagner, F. H., et al. (2018). 21st Century drought-related fires counteract the decline of Amazon deforestation carbon emissions. *Nat. Commun.* 9, 536. doi:10.1038/s41467-017-02771-y.

Aragão, L. E. O. C., Jiménez, E., Silva-Espejo, J. E., Costa, A. C. L., Monteagudo, A., Phillips, O. L., et al. (2010). Above- and below-ground net primary productivity across ten Amazonian forests on contrasting soils. *Biogeosciences Discuss.* 6, 2441–2488. doi:10.5194/bgd-6-2441-2009.

Assis, T. O., de Aguiar, A. P. D., von Randow, C., Melo de Paula Gomes, D., Kury, J. N., Ometto, J. P. H. B., et al. (2020). CO 2 emissions from forest degradation in Brazilian Amazon. *Environ. Res. Lett.* 15, 104035. doi:10.1088/1748-9326/ab9cfc.

Baccini, A., Walker, W., Carvalho, L., Farina, M., Sulla-Menashe, D., and Houghton, R. A. (2017). Tropical forests are a net carbon source based on aboveground measurements of gain and loss. *Science (80–. ).* 358, 230–234. doi:10.1126/science.aam5962.

Berner, L. T., Massey, R., Jantz, P., Forbes, B. C., Macias-Fauria, M., Myers-Smith, I., et al. (2020). Summer warming explains widespread but not uniform greening in the Arctic tundra biome. *Nat. Commun.* 11, 4621. doi:10.1038/s41467-020-18479-5.

Brinck, K., Fischer, R., Groeneveld, J., Lehmann, S., Dantas De Paula, M., Pütz, S., et al. (2017). High resolution analysis of tropical forest fragmentation and its impact on the global carbon cycle. *Nat. Commun.* 8, 14855. doi:10.1038/ncomms14855.

Brown, D. S., Brown, J. C., and Brown, C. (2016). Land occupations and deforestation in the Brazilian Amazon. *Land use policy* 54, 331–338. doi:10.1016/j.landusepol.2016.02.003.

Buermann, W., Forkel, M., O'Sullivan, M., Sitch, S., Friedlingstein, P., Haverd, V., et al. (2018). Widespread seasonal compensation effects of spring warming on northern plant productivity. *Nature* 562, 110–114. doi:10.1038/s41586-018-0555-7.

Bullock, E. L., Woodcock, C. E., Souza, C., and Olofsson, P. (2020). Satellite-based estimates reveal widespread forest degradation in the Amazon. *Glob. Chang. Biol.* 26, 2956–2969. doi:10.1111/gcb.15029.

Buras, A., Schunk, C., Zeitrg, C., Herrmann, C., Kaiser, L., Lemme, H., et al. (2018). Are Scots pine forest edges particularly prone to drought-induced mortality? *Environ. Res. Lett.* 13. doi:10.1088/1748-9326/aaa0b4.

Cabral, A. I. R., Saito, C., Pereira, H., and Laques, A. E. (2018). Deforestation pattern dynamics in protected areas of the Brazilian Legal Amazon using remote sensing data. *Appl. Geogr.* 100, 101–115. doi:10.1016/j.apgeog.2018.10.003.

Ceccherini, G., Duveiller, G., Grassi, G., Lemoine, G., and Avitabile, V. (2020). Abrupt Increase in Forest Harvested Area over Europe After 2015. *Nature* 583, 72–77. doi:10.1038/s41586-020-2438-y.

Chaplin-Kramer, R., Ramler, I., Sharp, R., Haddad, N. M., Gerber, J. S., West, P. C., et al. (2015). Degradation in carbon stocks near tropical forest edges. *Nat. Commun.* 6, 1–6. doi:10.1038/ncomms10158.

Cheng, L., Zhang, L., Wang, Y. P., Canadell, J. G., Chiew, F. H. S., Beringer, J., et al. (2017). Recent increases in terrestrial carbon uptake at little cost to the water cycle. *Nat. Commun.* 8. doi:10.1038/s41467-017-00114-5.

Cochrane, M. A. (2003). Review article: Fire science for rainforests. *Nature* 421, 913–919.

Copernicus Land Monitoring Service (2018). Corine land cover legend. *Eur. Environ. Agency*.

Cornes, R. C., van der Schrier, G., van den Besselaar, E. J. M., and Jones, P. D. (2018). An Ensemble Version of the E-OBS Temperature and Precipitation Data Sets. *J. Geophys. Res. Atmos.* 123, 9391–9409. doi:10.1029/2017JD028200.

Cox, P. M., Harris, P. P., Huntingford, C., Betts, R. A., Collins, M., Jones, C. D., et al. (2008). Increasing risk of Amazonian drought due to decreasing aerosol pollution. *Nature* 453, 212–5. doi:10.1038/nature06960.

Curtis, P. G., Slay, C. M., Harris, N. L., Tyukavina, A., and Hansen, M. C. (2018). Classifying drivers of global forest loss. *Science (80–. ).* 361, 1108–1111. doi:10.1126/science.aau3445.

De Kauwe, M. G., Medlyn, B. E., Pitman, A. J., Drake, J. E., Ukkola, A., Griebel, A., et al. (2019). Examining the evidence for decoupling between photosynthesis and transpiration during heat extremes. *Biogeosciences* 16, 903–916. doi:10.5194/bg-16-903-2019.

Dekker, S. C., Groenendijk, M., Booth, B. B. B., Huntingford, C., and Cox, P. M. (2016). Spatial and temporal variations in plant water-use efficiency inferred from tree-ring, eddy covariance and atmospheric observations. *Earth Syst. Dyn.* 7, 525–533. doi:10.5194/esd-7-525-2016.

Dias, L. C. P., Macedo, M. N., Costa, M. H., Coe, M. T., and Neill, C. (2015). Effects of land cover change on evapotranspiration and streamflow of small catchments in the Upper Xingu River Basin, Central Brazil. *J. Hydrol. Reg. Stud.* 4, 108–122. doi:10.1016/j.ejrh.2015.05.010.

Díaz, S., Settele, J., Brondízio, E. S., Ngo, H. T., Agard, J., Arneth, A., et al. (2019). Pervasive human-driven decline of life on Earth points to the need for transformative change. *Science (80–. ).* 366. doi:10.1126/science.aax3100.

dos Santos, C. A. C., Mariano, D. A., das Chagas A. do Nascimento, F., Fabiane, F. R., de Oliveira, G., Silva, M. T., et al. (2020). Spatio-temporal patterns of energy exchange and evapotranspiration during an intense drought for drylands in Brazil. *Int. J. Appl. Earth Obs. Geoinf.* 85, 101982. doi:10.1016/j.jag.2019.101982.

Dragoni, D., and Rahman, A. F. (2012). Trends in fall phenology across the deciduous forests of the Eastern USA. *Agric. For. Meteorol.* 157, 96–105. doi:10.1016/ j.agrformet.2012.01.019.

Duffy, K. A., Schwalm, C. R., Arcus, V. L., Koch, G. W., Liang, L. L., and Schipper, L. A. (2021). How close are we to the temperature tipping point of the terrestrial biosphere? *Sci. Adv.* 7, 1–9. doi:10.1126/sciadv.aay1052.

Ellison, D., Morris, C. E., Locatelli, B., Sheil, D., Cohen, J., Murdiyarso, D., et al. (2017). Trees, forests and water: Cool insights for a hot world. *Glob. Environ. Chang.* 43, 51–61. doi:10.1016/j.gloenvcha.2017.01.002.

FAO (2011). Assessing forest degradation: Towards the development of globally applicable guidlines. *For. Resour. Assess.*, 99.

Fearnside, P. M. (2005). Deforestation in Brazilian Amazonia: History, Rates, and Consequences. *Conserv. Biol.* 19, 680–688. doi:10.1111/j.1523-1739.2005.00697.x.

Findell, K. L., Berg, A., Gentine, P., Krasting, J. P., Lintner, B. R., Malyshev, S., et al. (2017). The impact of anthropogenic land use and land cover change on regional climate extremes. *Nat. Commun.* 8, 1–9. doi:10.1038/s41467-017-01038-w.

Fischer, R., Taubert, F., Müller, M. S., Groeneveld, J., Lehmann, S., Wiegand, T., et al. (2021). Accelerated forest fragmentation leads to critical increase in tropical forest edge area. *Sci. Adv.* 7, 1DUMMMY. doi:10.1126/sciadv.abg7012.

Fu, L., Xu, Y., Xu, Z., Wu, B., and Zhao, D. (2020). Tree water-use efficiency and growth dynamics in response to climatic and environmental changes in a temperate forest in Beijing, China. *Environ. Int.* 134. doi:10.1016/j.envint.2019.105209.

Gaertner, B. A., Zegre, N., Warner, T., Fernandez, R., He, Y., and Merriam, E. R. (2019). Climate, forest growing season, and evapotranspiration changes in the central Appalachian Mountains, USA. *Sci. Total Environ.* 650, 1371–1381. doi:10.1016/ j.scitotenv.2018.09.129.

Gao, Y., Skutsch, M., Paneque-Gálvez, J., and Ghilardi, A. (2020). Remote sensing of forest degradation: a review. *Environ. Res. Lett.* 15, 103001. doi:10.1088/1748-9326/ abaad7.

Gibbs, H. K., Rausch, L., Munger, J., Schelly, I., Morton, D. C., Noojipady, P., et al. (2015). Brazil's Soy Moratorium. *Science (80–. ).* 347, 377–378. doi:10.1126/ science.aaa0181.

Gollnow, F., Hissa, L. de B. V., Rufin, P., and Lakes, T. (2018). Property-level direct and indirect deforestation for soybean production in the Amazon region of Mato Grosso, Brazil. *Land use policy* 78, 377–385. doi:10.1016/j.landusepol.2018.07.010.

Grassi, G., House, J., Dentener, F., Federici, S., den Elzen, M., and Penman, J. (2017). The key role of forests in meeting climate targets requires science for credible mitigation. *Nat. Clim. Chang.* 7, 220–226. doi:10.1038/nclimate3227.

Griscom, B. W., Busch, J., Cook-Patton, S. C., Ellis, P. W., Funk, J., Leavitt, S. M., et al. (2020). National mitigation potential from natural climate solutions in the tropics. *Philos. Trans. R. Soc. B Biol. Sci.* 375. doi:10.1098/rstb.2019.0126.

Guerrieri, R., Belmecheri, S., Ollinger, S. V., Asbjornsen, H., Jennings, K., Xiao, J., et al. (2019). Disentangling the role of photosynthesis and stomatal conductance on rising forest water-use efficiency. *Proc. Natl. Acad. Sci. U. S. A.* 116, 16909–16914. doi:10.1073/pnas.1905912116.

Guerrieri, R., Vanguelova, E., Pitman, R., Benham, S., Perks, M., Morison, J. I. L., et al. (2020). Climate and atmospheric deposition effects on forest water-use efficiency and nitrogen availability across Britain. *Sci. Rep.* 10, 1–16. doi:10.1038/s41598-020-67562-w.

Guo, D., Westra, S., and Maier, H. R. (2017). Sensitivity of potential evapotranspiration to changes in climate variables for different Australian climatic zones. *Hydrol. Earth Syst. Sci.* 21, 2107–2126. doi:10.5194/hess-21-2107-2017.

Haddad, N. M., Brudvig, L. A., Clobert, J., Davies, K. F., Gonzalez, A., Holt, R. D., et al. (2015). Habitat fragmentation and its lasting impact on Earth's ecosystems. *Sci. Adv.* 1, 1–10. doi:10.1126/sciadv.1500052.

Hansen, M. C., Potapov, P. V, Moore, R., Hancher, M., Turubanova, S. A., and Tyukavina, A. (2013). High-Resolution Global Maps of 21st-Century Forest Cover Change. *Science (80–. ).* 342 (6160), 850–853.

Harris, N. L., Gibbs, D. A., Baccini, A., Birdsey, R. A., de Bruin, S., Farina, M., et al. (2021). Global maps of twenty-first century forest carbon fluxes. *Nat. Clim. Chang.* doi:10.1038/s41558-020-00976-6.

Harris, N. L., Goldman, E., Gabris, C., Nordling, J., Minnemeyer, S., Ansari, S., et al. (2017). Using spatial statistics to identify emerging hot spots of forest loss. *Environ. Res. Lett.* 12.

Harrison, J. L., Sanders-DeMott, R., Reinmann, A. B., Sorensen, P. O., Phillips, N. G., and Templer, P. H. (2020). Growing-season warming and winter soil freeze/thaw cycles increase transpiration in a northern hardwood forest. *Ecology* 101, 1–16. doi:10.1002/ecy.3173.

Hatfield, J. L., and Dold, C. (2019). Water-use efficiency: Advances and challenges in a changing climate. *Front. Plant Sci.* 10, 1–14. doi:10.3389/fpls.2019.00103.

Heinrich, V. H. A., Dalagnol, R., Cassol, H. L. G., Rosan, T. M., Torres, C., Almeida, D., et al. (2017). Large carbon sink potential of Amazonian Secondary Forests to mitigate climate change. *Natures Res.* 1, 4–6. doi:10.1038/s41467-021-22050-1.

Holden, Z. A., Swanson, A., Luce, C. H., Jolly, W. M., Maneta, M., Oyler, J. W., et al. (2018). Decreasing fire season precipitation increased recent western US forest wildfire activity. *Proc. Natl. Acad. Sci. U. S. A.* 115, E8349–E8357. doi:10.1073/pnas.1802316115.

INPE (2016). INPE-PRODES – Projeto de Monitoramento do Desmatamento na Amazônia Brasileira por Satélite.

Ionita, M., Nagavciuc, V., Kumar, R., and Rakovec, O. (2020). On the curious case of the recent decade, mid-spring precipitation deficit in central Europe. *npj Clim. Atmos. Sci.* 3, 1–10. doi:10.1038/s41612-020-00153-8.

IPCC (2019). IPCC Special Report on Climage Change and Land: Chapter 4: Land Degradation. 1–112. Available at: https://www.ipcc.ch/report/srccl/.

Jaagus, J., Sepp, M., Tamm, T., Järvet, A., and Mõisja, K. (2017). Trends and regime shifts in climatic conditions and river runoff in Estonia during 1951–2015. *Earth Syst. Dyn.* 8, 963–976. doi:10.5194/esd-8-963-2017.

Jaagus, J., Truu, J., Ahas, R., and Aasa, A. (2003). Spatial and temporal variability of climatic seasons on the East European Plain in relation to large-scale atmospheric circulation. *Clim. Res.* 23, 111–129. doi:10.3354/cr023111.

Jiang, Y., Still, C. J., Rastogi, B., Page, G. F. M., Wharton, S., Meinzer, F. C., et al. (2019). Trends and controls on water-use efficiency of an old-growth coniferous forest in the Pacific Northwest. *Environ. Res. Lett.* 14. doi:10.1088/1748-9326/ab2612.

Jiménez-Muñoz, J. C., Mattar, C., Barichivich, J., Santamaría-Artigas, A., Takahashi, K., Malhi, Y., et al. (2016). Record-breaking warming and extreme drought in the Amazon rainforest during the course of El Niño 2015–2016. *Sci. Rep.* 6, 1–7. doi:10.1038/srep33130.

Kalamandeen, M., Gloor, E., Mitchard, E., Quincey, D., Ziv, G., Spracklen, D., et al. (2018). Pervasive Rise of Small-scale Deforestation in Amazonia. *Sci. Rep.* 8, 1600. doi:10.1038/s41598-018-19358-2.

Keenan, T. F., Gray, J., Friedl, M. A., Toomey, M., Bohrer, G., Hollinger, D. Y., et al. (2014). Net carbon uptake has increased through warming-induced changes in temperate forest phenology. *Nat. Clim. Chang.* 4, 598–604. doi:10.1038/nclimate2253.

Keller, M., Knapp, D. E., Asner, G. P., Silva, J. N., Oliveira, P. J. C., and Broadbent, E. N. (2008). Forest fragmentation and edge effects from deforestation and selective logging in the Brazilian Amazon. *Biol. Conserv.* 141, 1745–1757. doi:10.1016/j.biocon.2008.04.024.

Kendall, M. G. (1957). Rank Correlation Methods. *Biometrika* 44, 298. doi:10.2307/2333282.

Knauer, J., Zaehle, S., Reichstein, M., Medlyn, B. E., Forkel, M., Hagemann, S., et al. (2017). The response of ecosystem water-use efficiency to rising atmospheric CO2 concentrations: sensitivity and large-scale biogeochemical implications. *New Phytol.* 213, 1654–1666. doi:10.1111/nph.14288.

Kriauciuniene, J., Meilutyte-Barauskiene, D., Reihan, A., Koltsova, T., Lizuma, L., and Sarauskiene, D. (2012). Variability in temperature, precipitation and river discharge in the Baltic States. *Boreal Environ. Res.* 17, 150–162.

Laurance, W. F., Camargo, J. L. C., Luizão, R. C. C., Laurance, S. G., Pimm, S. L., Bruna, E. M., et al. (2011). The fate of Amazonian forest fragments: A 32-year investigation. *Biol. Conserv.* 144, 56–67. doi:10.1016/j.biocon.2010.09.021.

Law, B. E., Hudiburg, T. W., Berner, L. T., Kent, J. J., Buotte, P. C., and Harmon, M. E. (2018). Land use strategies to mitigate climate change in carbon dense temperate forests. *Proc. Natl. Acad. Sci. U. S. A.* 115, 3663–3668. doi:10.1073/pnas.1720064115.

Li, G., Zhang, F., Jing, Y., Liu, Y., and Sun, G. (2017). Response of evapotranspiration to changes in land use and land cover and climate in China during 2001–2013. *Sci. Total Environ.* 596–597, 256–265. doi:10.1016/j.scitotenv.2017.04.080.

Lian, X., Piao, S., Li, L. Z. X., Li, Y., Huntingford, C., Ciais, P., et al. (2020). Summer soil drying exacerbated by earlier spring greening of northern vegetation. *Sci. Adv.* 6, eaax0255. doi:10.1126/sciadv.aax0255.

Lima, A., Silva, T. S. F., de Aragão, L. E. O. e. C., de Feitas, R. M., Adami, M., Formaggio, A. R., et al. (2012). Land use and land cover changes determine the spatial relationship between fire and deforestation in the Brazilian Amazon. *Appl. Geogr.* 34, 239–246. doi:10.1016/j.apgeog.2011.10.013.

Lindroth, A., Holst, J., Heliasz, M., Vestin, P., Lagergren, F., Biermann, T., et al. (2018). Effects of low thinning on carbon dioxide fluxes in a mixed hemiboreal forest. *Agric. For. Meteorol.* 262, 59–70. doi:10.1016/j.agrformet.2018.06.021.

Liu, J., You, Y., Li, J., Sitch, S., Gu, X., Nabel, J. E. M. S., et al. (2021). Response of global land evapotranspiration to climate change, elevated CO2, and land use change. *Agric. For. Meteorol.* 311, 108663. doi:10.1016/j.agrformet.2021.108663.

Makarieva, A. M., Gorshkov, V. G., and Li, B. L. (2013). Revisiting forest impact on atmospheric water vapor transport and precipitation. *Theor. Appl. Climatol.* 111, 79–96. doi:10.1007/s00704-012-0643-9.

Malhi, Y., Aragão, L. E. O. C., Metcalfe, D. B., Paiva, R., Quesada, C. A., Almeida, S., et al. (2009). Comprehensive assessment of carbon productivity, allocation and storage in three Amazonian forests. *Glob. Chang. Biol.* 15, 1255–1274. doi:10.1111/j.1365-2486.2008.01780.x.

Mann, H. B. (1945). Non-Parametric Test Against Trend. *Econometrica* 13, 245–259. Available at: http://www.economist.com/node/18330371?story%7B_%7Did=18330371.

Marengo, J. A. (2004). Interdecadal variability and trends of rainfall across the Amazon basin. *Theor. Appl. Climatol.* 78, 79–96. doi:10.1007/s00704-004-0045-8.

Marshall, M., Okuto, E., Kang, Y., Opiyo, E., and Ahmed, M. (2016). Global assessment of Vegetation Index and Phenology Lab (VIP) and Global Inventory Modeling and Mapping Studies (GIMMS) version 3 products. *Biogeosciences* 13, 625–639. doi:10.5194/bg-13-625-2016.

Matricardi, E. A. T., Skole, D. L., Costa, O. B., Pedlowski, M. A., Samek, J. H., and Miguel, E. P. (2020). Long-term forest degradation surpasses deforestation in the Brazilian Amazon. *Science (80–. ).* 369, 1378–1382. doi:10.1126/SCIENCE.ABB3021.

McDowell, N. G., Allen, C. D., Anderson-Teixeira, K., Aukema, B. H., Bond-Lamberty, B., Chini, L., et al. (2020). Pervasive shifts in forest dynamics in a changing world. *Science (80–. ).* 368. doi:10.1126/science.aaz9463.

Mu, Q., Zhao, M., and Running, S. W. (2011). Improvements to a MODIS global terrestrial evapotranspiration algorithm. *Remote Sens. Environ.* 115, 1781–1800. doi:10.1016/j.rse.2011.02.019.

Nepstad, D., McGrath, D., Stickler, C., Alencar, A., Azevedo, A., Swette, B., et al. (2014). Slowing Amazon deforestation through public policy and interventions in beef and soy supply chains. *Science (80–. ).* 344, 1118–1123. doi:10.1126/science.1248525.

Nolan, C., Overpeck, J. T., Allen, J. R. M., Anderson, P. M., Betancourt, J. L., Binney, H. A., et al. (2018). Past and future global transformation of terrestrial ecosystems under climate change. *Science (80–. ).* 361, 920–923. doi:10.1126/science.aan5360.

Ordway, E. M., and Asner, G. P. (2020). Carbon declines along tropical forest edges correspond to heterogeneous effects on canopy structure and function. *Proc. Natl. Acad. Sci. U. S. A.* 117, 7863–7870. doi:10.1073/pnas.1914420117.

Paca, V. H. da M., Espinoza-Dávalos, G. E., Hessels, T. M., Moreira, D. M., Comair, G. F., and Bastiaanssen, W. G. M. (2019). The spatial variability of actual evapotranspiration across the Amazon River Basin based on remote sensing products validated with flux towers. *Ecol. Process.* 8. doi:10.1186/s13717-019-0158-8.

Palareti, G., Legnani, C., Cosmi, B., Antonucci, E., Erba, N., Poli, D., et al. (2016). *Comparison between different D-Dimer cutoff values to assess the individual risk of recurrent venous thromboembolism: Analysis of results obtained in the DULCIS study*. doi:10.1111/ijlh.12426.

Parente, L., Witjes, M. , Hengl, T., Landa, M., Brodsky, L. (2021). Continental Europe land cover mapping at 30m resolution based CORINE and LUCAS on samples. doi:10.5281/zenodo.4725429.

Pearson, T. R. H., Brown, S., Murray, L., and Sidman, G. (2017). Greenhouse gas emissions from tropical forest degradation: An underestimated source. *Carbon Balance Manag.* 12. doi:10.1186/s13021-017-0072-2.

Perugini, L., Caporaso, L., Marconi, S., Cescatti, A., Quesada, B., De Noblet-Ducoudré, N., et al. (2017). Biophysical effects on temperature and precipitation due to land cover change. *Environ. Res. Lett.* 12. doi:10.1088/1748-9326/aa6b3f.

Poon, P. K., and Kinoshita, A. M. (2018). Spatial and temporal evapotranspiration trends after wildfire in semi-arid landscapes. *J. Hydrol.* 559, 71–83. doi:10.1016/j.jhydrol.2018.02.023.

Potapov, P., Hansen, M. C., Laestadius, L., Turubanova, S., Yaroshenko, A., Thies, C., et al. (2017). The last frontiers of wilderness: Tracking loss of intact forest landscapes from 2000 to 2013. *Sci. Adv.* 3, e1600821. doi:10.1126/sciadv.1600821.

Pugh, T. A. M., Lindeskog, M., Smith, B., Poulter, B., Arneth, A., Haverd, V., et al. (2019). Role of forest regrowth in global carbon sink dynamics. *Proc. Natl. Acad. Sci. U. S. A.* 116, 4382–4387. doi:10.1073/pnas.1810512116.

Puhlick, J. J., Weiskittel, A. R., Kenefic, L. S., Woodall, C. W., and Fernandez, I. J. (2020). Strategies for enhancing long-term carbon sequestration in mixed-species, naturally regenerated Northern temperate forests. *Carbon Manag.* 11, 381–397. doi:10.1080/17583004.2020.1795599.

Qin, Y., Xiao, X., Wigneron, J. P., Ciais, P., Brandt, M., Fan, L., et al. (2021). Carbon loss from forest degradation exceeds that from deforestation in the Brazilian Amazon. *Nat. Clim. Chang.* 11, 442–448. doi:10.1038/s41558-021-01026-5.

República, C. C. da P. da (2004). Plano de Acao para a Prevencao e Controle do Desmatamento na Amazonia Legal. 156.

Richards, P., Arima, E., VanWey, L., Richards, P., Bhattarai, N., and Cohn, A. (2016). Are Brazil's deforesters avoiding detection? *Conserv. Lett.* 10, 470–476. doi:10.1111/conl.12310.

Rosa, I. M. D., Souza, C., and Ewers, R. M. (2012). Changes in size of deforested patches in the Brazilian Amazon. *Conserv. Biol.* 26, 932–937. doi:10.1111/j.1523-1739.2012.01901.x.

Rudorff, B. F. T., Amaral, D. F., Fabiani, L., Aguiar, D. A., Rudorff, B. F. T., Mello, M. P., et al. (2011). The Soy Moratorium in the Amazon biome monitored by remote sensing Images. *Remote Sens.* 3, 185–202. doi:10.3390/rs3010185.

Running, S. W., Nemani, R. R., Heinsch, F. A., Zhao, M., Reeves, M., and Hashimoto, H. (2004). A continuous satellite-derived measure of global terrestrial primary production. *Bioscience* 54, 547–560. doi:10.1641/0006-3568(2004)054[0547: ACSMOG]2.0.CO;2.

Schelhaas, M. J., Nabuurs, G. J., Hengeveld, G., Reyer, C., Hanewinkel, M., Zimmermann, N. E., et al. (2015). Alternative forest management strategies to account for climate change-induced productivity and species suitability changes in Europe. *Reg. Environ. Chang.* 15, 1581–1594. doi:10.1007/s10113-015-0788-z.

Schlesinger, W. H., and Jasechko, S. (2014). Transpiration in the global water cycle. *Agric. For. Meteorol.* 189–190, 115–117. doi:10.1016/j.agrformet.2014.01.011.

Schneider, M., and Peres, C. A. (2015). Environmental costs of government-sponsored agrarian settlements in Brazilian Amazonia. *PLoS One* 10, 1–23. doi:10.1371/journal.pone.0134016.

Seddon, A. W. R., Macias-Fauria, M., Long, P. R., Benz, D., and Willis, K. J. (2016). Sensitivity of global terrestrial ecosystems to climate variability. *Nature* 531, 229–232. doi:10.1038/nature16986.

Seneviratne, S. I., Nicholls, N., Easterling, D., Goodess, C. M., Kanae, S., Kossin, J., et al. (2012). Changes in climate extremes and their impacts on the natural physical environment. *Manag. Risks Extrem. Events Disasters to Adv. Clim. Chang. Adapt. Spec. Rep. Intergov. Panel Clim. Chang.* 9781107025, 109–230. doi:10.1017/CBO9781139177245.006.

Senf, C., and Seidl, R. (2020). Mapping the forest disturbance regimes of Europe. *Nat. Sustain.* doi:10.1038/s41893-020-00609-y.

Silva, C. H. L., Aragão, L. E. O. C., Anderson, L. O., Fonseca, M. G., Shimabukuro, Y. E., Vancutsem, C., et al. (2020). Persistent collapse of biomass in Amazonian forest edges following deforestation leads to unaccounted carbon losses. *Sci. Adv.* 6, 1–10. doi:10.1126/sciadv.aaz8360.

Silva, S. S. da, Fearnside, P. M., Graça, P. M. L. de A., Brown, I. F., Alencar, A., and Melo, A. W. F. de (2018). Dynamics of forest fires in the southwestern Amazon. *For. Ecol. Manage.* 424, 312–322. doi:10.1016/j.foreco.2018.04.041.

Sippel, S., Forkel, M., Rammig, A., Thonicke, K., Flach, M., Heimann, M., et al. (2017). Contrasting and interacting changes in simulated spring and summer carbon cycle extremes in European ecosystems. *Environ. Res. Lett.* 12. doi:10.1088/1748-9326/aa7398.

Spera, S. A., Galford, G. L., Coe, M. T., Macedo, M. N., and Mustard, J. F. (2016). Land-use change affects water recycling in Brazil's last agricultural frontier. *Glob. Chang. Biol.* 22, 3405–3413. doi:10.1111/gcb.13298.

Sperlich, D., Nadal-Sala, D., Gracia, C., Kreuzwieser, J., Hanewinkel, M., and Yousefpour, R. (2020). Gains or losses in forest productivity under climate change? The uncertainty of CO2 fertilization and climate effects. *Climate* 8, 1–22. doi:10.3390/cli8120141.

Staal, A., Tuinenburg, O. A., Bosmans, J. H. C., Holmgren, M., Van Nes, E. H., Scheffer, M., et al. (2018). Forest-rainfall cascades buffer against drought across the Amazon. *Nat. Clim. Chang.* 8, 539–543. doi:10.1038/s41558-018-0177-y.

Sy, S., and Quesada, B. (2020). Anthropogenic land cover change impact on climate extremes during the 21st century. *Environ. Res. Lett.* 15. doi:10.1088/1748-9326/ab702c.

Tang, J., Luyssaert, S., Richardson, A. D., Kutsch, W., and Janssens, I. A. (2014). Steeper declines in forest photosynthesis than respiration explain age-driven decreases in forest growth. *Proc. Natl. Acad. Sci. U. S. A.* 111, 8856–8860. doi:10.1073/pnas.1320761111.

Taubert, F., Fischer, R., Groeneveld, J., Lehmann, S., Müller, M. S., Rödig, E., et al. (2018). Global patterns of tropical forest fragmentation. *Nature* 554, 519–522. doi:10.1038/nature25508.

Teuling, A. J., De Badts, E. A. G., Jansen, F. A., Fuchs, R., Buitink, J., Van Dijke, A. J. H., et al. (2019). Climate change, reforestation/afforestation, and urbanization impacts on evapotranspiration and streamflow in Europe. *Hydrol. Earth Syst. Sci.* 23, 3631–3652. doi:10.5194/hess-23-3631-2019.

Trenberth, K. E., Dai, A., Van Der Schrier, G., Jones, P. D., Barichivich, J., Briffa, K. R., et al. (2014). Global warming and changes in drought. *Nat. Clim. Chang.* 4, 17–22. doi:10.1038/nclimate2067.

Van Schaik, E., Killaars, L., Smith, N. E., Koren, G., Van Beek, L. P. H., Peters, W., et al. (2018). Changes in surface hydrology, soil moisture and gross primary production in the Amazon during the 2015/2016 El Niño. *Philos. Trans. R. Soc. B Biol. Sci.* 373. doi:10.1098/rstb.2018.0084.

Vedovato, L. B., Fonseca, M. G., Arai, E., Anderson, L. O., and Aragão, L. E. O. C. (2016). The extent of 2014 forest fragmentation in the Brazilian Amazon. *Reg. Environ. Chang.* 16, 2485–2490. doi:10.1007/s10113-016-1067-3.

Vourlitis, G. L., de Souza Nogueira, J., de Almeida Lobo, F., and Pinto, O. B. (2014). Variations in evapotranspiration and climate for an Amazonian semi-deciduous forest over seasonal, annual, and El Niño cycles. *Int. J. Biometeorol.* 59, 217–230. doi:10.1007/s00484-014-0837-1.

Wang, M., Chen, Y., Wu, X., and Bai, Y. (2018). Forest-Type-Dependent Water Use Efficiency Trends Across the Northern Hemisphere. *Geophys. Res. Lett.* 45, 8283–8293. doi:10.1029/2018GL079093.

Wolf, S., Keenan, T. F., Fisher, J. B., Baldocchi, D. D., Desai, A. R., Richardson, A. D., et al. (2016). Warm spring reduced carbon cycle impact of the 2012 US summer drought. *Proc. Natl. Acad. Sci. U. S. A.* 113, 5880–5885. doi:10.1073/pnas.1519620113.

Xu, X., Zhang, X., Riley, W. J., Xue, Y., Nobre, C. A., Lovejoy, T. E., et al. (2022). Deforestation triggering irreversible transition in Amazon hydrological cycle. *Environ. Res. Lett.* 17, 034037. doi:10.1088/1748-9326/ac4c1d.

Yang, J., Tian, H., Pan, S., Chen, G., Zhang, B., and Dangal, S. (2018). Amazon drought and forest response: Largely reduced forest photosynthesis but slightly increased canopy greenness during the extreme drought of 2015/2016. *Glob. Chang. Biol.* 24, 1919–1934. doi:10.1111/gcb.14056.

Zhang, Y., Peña-Arancibia, J. L., McVicar, T. R., Chiew, F. H. S., Vaze, J., Liu, C., et al. (2016). Multi-decadal trends in global terrestrial evapotranspiration and its components. *Sci. Rep.* 6, 1–12. doi:10.1038/srep19124.

Zhao, M., Heinsch, F. A., Nemani, R. R., and Running, S. W. (2005). Improvements of the MODIS terrestrial gross and net primary production global data set. *Remote Sens. Environ.* 95, 164–176. doi:10.1016/j.rse.2004.12.011.

Zohner, C. M., Mo, L., Pugh, T. A. M., Bastin, J. F., and Crowther, T. W. (2020). Interactive climate factors restrict future increases in spring productivity of temperate and boreal trees. *Glob. Chang. Biol.* 26, 4042–4055. doi:10.1111/gcb.15098.

# PUBLICATIONS

# CURRICULUM VITAE

**Name:** Bruno Montibeller
**Date of birth:** 21.06.1993
**E-mail:** bruno.montibeller@ut.ee

**Education:**

| | |
|---|---|
| 2018–present | PhD in Geoinformatics, Department of Geography, University of Tartu, Estonia |
| 2016–2018 | MSc in Remote Sensing, National Institute for Space Research, Brazil |
| 2011–2015 | BSc in Geography, Federal University of Santa Catarina, Brazil |

**Work experience:**

| | |
|---|---|
| 2016–2018 | National Institute for Space Research-INPE, Research member |
| 2014–2016 | Agrostalite ltd, GIS and remote sensing analyst |

**Scholarships:**

| | |
|---|---|
| 2018–2022 | Smart specialisation scholarships for entrepreneurial PhD students |

**Publications:**

**Montibeller**, B., Marshall, M., Mander, U.,Uuemaa, E., 2022. Increased carbon assimilation and efficient water usage may not compensate for carbon loss in European forests. Communications Earth & Environment, 3(1), p. 1-11. https://doi.org/10.1038/s43247-022-00535-1.

**Montibeller**, B., Jaagus, J., Mander, U.,Uuemaa, E., 2021. Evapotranspiration Intensification Over Unchanged Temperate Vegetation in the Baltic Countries Is Being Driven by Climate Shifts. Frontiers in Forests and Global Change, 4, ARTN 663327. https://doi.org/10.3389/ffgc.2021.663327

Uuemaa, E., Ahi, S., **Montibeller, B.,** Muru, M. and Kmoch, A., 2020. Vertical accuracy of freely available global digital elevation models (ASTER, AW3D30, MERIT, TanDEM-X, SRTM, and NASADEM). Remote Sensing, 12(21), p. 3482. https://doi.org/10.3390/rs12213482

**Montibeller, B.,** Kmoch, A., Virro, H., Mander, Ü. and Uuemaa, E., 2020. Increasing fragmentation of forest cover in Brazil's Legal Amazon from 2001 to 2017. *Scientific reports*, 10(1), pp. 1–13. https://doi.org/10.1038/s41598-020-62591-x

Sanches, I.D., Feitosa, R.Q., **Montibeller, B**., Diaz, P.A., Luiz, A.J.B., Soares, M.D., Prudente, V.H.R., Vieira, D.C., Maurano, L.E.P., Happ, P.N. and Chamorro, J., 2020. First Results Of The Lem Benchmark Database For

Agricultural Applications. *The International Archives of Photogrammetry, Remote Sensing and Spatial Information Sciences*, *43*, pp. 251–256. https://doi.org/10.5194/isprs-archives-XLIII-B5-2020-251-2020

**Montibeller, B.,** Sanches, I., Luiz, A.J.B., Gonçalves, F. and de Aguiar, D.A., 2019. Spectraltemporal profile analysis of maize, soybean and sugarcane based on OLI/Landsat-8 data. *Brazilian Journal of Agriculture*. https://doi.org/10.37856/bja.v94i3.

Sanches, I. D., Luiz, A. J. B., **Montibeller, B.,** Schultz, B., Trabaquini, K., Eberhardt, I. D. R., Formaggio, A. R., and Maurano, L. E., 2019. Understanding the Dynamic of Tropical Agriculture for Remote Sensing Applications: A Case Study of Southeastern Brazil, *The International Archives of Photogrammetry, Remote Sensing and Spatial Information Sciences*, https://doi.org/10.5194/isprs-archives-XLII-3-W6-149-2019

# ELULOOKIRJELDUS

**Nimi:** Bruno Montibeller
**Sünniaeg:** 21.06.1993
**E-mail:** bruno.montibeller@ut.ee

**Haridustee:**

| | |
|---|---|
| 2018–… | PhD geoinformaatika erialal, Tartu Ülikool |
| 2016–2018 | MSc kaugseires, Brasiila Riiklik Kosmoseuuringute Instituut (INPE) |
| 2011–2015 | BSc geograafias, Santa Catarina Riiklik Ülikool, Brasiilia |

**Töökogemus:**

| | |
|---|---|
| 2016–2018 | Brasiilia Riiklik Kosmoseuuringute Instituut, teadur |
| 2014–2016 | Agrostalite ltd, GIS ja kaugseire analüütik |

**Stipendiumid:**

2018–2022 nutikas spetsialiseerumise stipendium NUTIKAS

**Publikatsioonid:**

**Montibeller**, B., Marshall, M., Mander, U.,Uuemaa, E., 2022. Increased carbon assimilation and efficient water usage may not compensate for carbon loss in European forests. Communications Earth & Environment, 3(1), p. 1–11. https://doi.org/10.1038/s43247-022-00535-1.

**Montibeller**, B., Jaagus, J., Mander, U.,Uuemaa, E., 2021. Evapotranspiration Intensification Over Unchanged Temperate Vegetation in the Baltic Countries Is Being Driven by Climate Shifts. Frontiers in Forests and Global Change, 4, ARTN 663327. https://doi.org/10.3389/ffgc.2021.663327

Uuemaa, E., Ahi, S., Montibeller, B., Muru, M. and Kmoch, A., 2020. Vertical accuracy of freely available global digital elevation models (ASTER, AW3D30, MERIT, TanDEM-X, SRTM, and NASADEM). Remote Sensing, 12(21), p.3482. https://doi.org/10.3390/rs12213482

**Montibeller, B.,** Kmoch, A., Virro, H., Mander, Ü. and Uuemaa, E., 2020. Increasing fragmentation of forest cover in Brazil's Legal Amazon from 2001 to 2017. *Scientific reports*, 10(1), pp. 1–13. https://doi.org/10.1038/s41598-020-62591-x

Sanches, I.D., Feitosa, R.Q., **Montibeller, B**., Diaz, P.A., Luiz, A.J.B., Soares, M.D., Prudente, V.H.R., Vieira, D.C., Maurano, L.E.P., Happ, P.N. and Chamorro, J., 2020. First Results Of The Lem Benchmark Database For Agricultural Applications. *The International Archives of Photogrammetry, Remote Sensing and Spatial Information Sciences*, *43*, pp. 251–256. https://doi.org/10.5194/isprs-archives-XLIII-B5-2020-251-2020

**Montibeller, B.,** Sanches, I., Luiz, A.J.B., Gonçalves, F. and de Aguiar, D.A., 2019. Spectraltemporal profile analysis of maize, soybean and sugarcane based on OLI/Landsat-8 data. *Brazilian Journal of Agriculture*. https://doi.org/10.37856/bja.v94i3.

Sanches, I. D., Luiz, A. J. B., **Montibeller, B.,** Schultz, B., Trabaquini, K., Eberhardt, I. D. R., Formaggio, A. R., and Maurano, L. E., 2019. Understanding the Dynamic of Tropical Agriculture for Remote Sensing Applications: A Case Study of Southeastern Brazil, *The International Archives of Photogrammetry, Remote Sensing and Spatial Information Sciences*, https://doi.org/10.5194/isprs-archives-XLII-3-W6-149-2019

# DISSERTATIONES GEOGRAPHICAE UNIVERSITATIS TARTUENSIS

1. **Вийви Руссак.** Солнечная радиация в Тыравере. Тарту, 1991.
2. **Urmas Peterson.** Studies on Reflectance Factor Dynamics of Forest Communities in Estonia. Tartu, 1993.
3. **Ülo Suursaar.** Soome lahe avaosa ja Eesti rannikumere vee kvaliteedi analüüs. Tartu, 1993.
4. **Kiira Aaviksoo.** Application of Markov Models in Investigation of Vegetation and Land Use Dynamics in Estonian Mire Landscapes. Tartu, 1993.
5. **Kjell Weppling.** On the assessment of feasible liming strategies for acid sulphate waters in Finland. Tartu, 1997.
6. **Hannes Palang.** Landscape changes in Estonia: the past and the future. Tartu, 1998.
7. **Eiki Berg.** Estonia's northeastern periphery in politics: socio-economic and ethnic dimensions. Tartu, 1999.
8. **Valdo Kuusemets.** Nitrogen and phosphorus transformation in riparian buffer zones of agricultural landscapes in Estonia. Tartu, 1999.
9. **Kalev Sepp.** The methodology and applications of agricultural landscape monitoring in Estonia. Tartu, 1999.
10. **Rein Ahas.** Spatial and temporal variability of phenological phases in Estonia. Tartu, 1999.
11. **Эркки Таммиксаар.** Географические аспекты творчества Карла Бэра в 1830–1840 гг. Тарту, 2000.
12. **Garri Raagmaa.** Regional identity and public leaders in regional economic development. Tartu, 2000.
13. **Tiit Tammaru.** Linnastumine ja linnade kasv Eestis nõukogude aastatel. Tartu, 2001.
14. **Tõnu Mauring.** Wastewater treatment weltlands in Estonia: efficiency and landscape analysis. Tartu, 2001.
15. **Ain Kull.** Impact of weather and climatic fluctuations on nutrient flows in rural catchments. Tartu, 2001.
16. **Robert Szava-Kovats.** Assessment of stream sediment contamination by median sum of weighted residuals regression. Tartu, 2001.
17. **Heno Sarv.** Indigenous Europeans east of Moscow. Population and Migration Patterns of the Largest Finno-Ugrian Peoples in Russia from the 18$^{th}$ to the 20$^{th}$ Centuries. Tartu, 2002.
18. **Mart Külvik.** Ecological networks in Estonia — concepts and applications. Tartu, 2002.
19. **Arvo Järvet.** Influence of hydrological factors and human impact on the ecological state of shallow Lake Võrtsjärv in Estonia. Tartu, 2004.
20. **Katrin Pajuste.** Deposition and transformation of air pollutants in coniferous forests. Tartu, 2004.

21. **Helen Sooväli.** *Saaremaa waltz*. Landscape imagery of Saaremaa Island in the 20th century. Tartu, 2004.
22. **Antti Roose.** Optimisation of environmental monitoring network by integrated modelling strategy with geographic information system — an Estonian case. Tartu, 2005.
23. **Anto Aasa.** Changes in phenological time series in Estonia and Central and Eastern Europe 1951–1998. Relationships with air temperature and atmospheric circulation. Tartu, 2005.
24. **Anneli Palo.** Relationships between landscape factors and vegetation site types: case study from Saare county, Estonia. Tartu, 2005.
25. **Mait Sepp.** Influence of atmospheric circulation on environmental variables in Estonia. Tartu, 2005.
26. **Helen Alumäe.** Landscape preferences of local people: considerations for landscape planning in rural areas of Estonia. Tartu, 2006.
27. **Aarne Luud.** Evaluation of moose habitats and forest reclamation in Estonian oil shale mining areas. Tartu, 2006.
28. **Taavi Pae.** Formation of cultural traits in Estonia resulting from historical administrative division. Tartu, 2006.
29. **Anneli Kährik.** Socio-spatial residential segregation in post-socialist cities: the case of Tallinn, Estonia. Tartu, 2006.
30. **Dago Antov.** Road user perception towards road safety in Estonia. Tartu, 2006.
31. **Üllas Ehrlich.** Ecological economics as a tool for resource based nature conservation management in Estonia. Tartu, 2007.
32. **Evelyn Uuemaa.** Indicatory value of landscape metrics for river water quality and landscape pattern. Tartu, 2007.
33. **Raivo Aunap.** The applicability of gis data in detecting and representing changes in landscape: three case studies in Estonia. Tartu, 2007.
34. **Kai Treier.** Trends of air pollutants in precipitation at Estonian monitoring stations. Tartu, 2008.
35. **Kadri Leetmaa.** Residential suburbanisation in the Tallinn metropolitan area. Tartu, 2008.
36. **Mare Remm.** Geographic aspects of enterobiasis in Estonia. Tartu, 2009.
37. **Alar Teemusk.** Temperature and water regime, and runoff water quality of planted roofs. Tartu, 2009.
38. **Kai Kimmel.** Ecosystem services of Estonian wetlands. Tartu, 2009.
39. **Merje Lesta.** Evaluation of regulation functions of rural landscapes for the optimal siting of treatment wetlands and mitigation of greenhouse gas emissions. Tartu, 2009.
40. **Siiri Silm.** The seasonality of social phenomena in Estonia: the location of the population, alcohol consumption and births. Tartu, 2009.
41. **Ene Indermitte.** Exposure to fluorides in drinking water and dental fluorosis risk among the population of Estonia. Tartu, 2010.
42. **Kaido Soosaar.** Greenhouse gas fluxes in rural landscapes of Estonia. Tartu, 2010.

43. **Jaan Pärn.** Landscape factors in material transport from rural catchments in Estonia. Tartu, 2010.
44. **Triin Saue.** Simulated potato crop yield as an indicator of climate variability in Estonia. Tartu, 2011.
45. **Katrin Rosenvald.** Factors affecting EcM roots and rhizosphere in silver birch stands. Tartu, 2011.
46. **Ülle Marksoo.** Long-term unemployment and its regional disparities in Estonia. Tartu, 2011, 163 p.
47. **Hando Hain.** The role of voluntary certification in promoting sustainable natural resource use in transitional economies. Tartu, 2012, 180 p.
48. **Jüri-Ott Salm.** Emission of greenhouse gases $CO_2$, $CH_4$, and $N_2O$ from Estonian transitional fens and ombrotrophic bogs: the impact of different land-use practices. Tartu, 2012, 125 p.
49. **Valentina Sagris.** Land Parcel Identification System conceptual model: development of geoinfo community conceptual model. Tartu, 2013, 161 p.
50. **Kristina Sohar.** Oak dendrochronology and climatic signal in Finland and the Baltic States. Tartu, 2013, 129 p.
51. **Riho Marja.** The relationships between farmland birds, land use and landscape structure in Northern Europe. Tartu, 2013, 134 p.
52. **Olle Järv.** Mobile phone based data in human travel behaviour studies: New insights from a longitudinal perspective. Tartu, 2013, 168 p.
53. **Sven-Erik Enno.** Thunderstorm and lightning climatology in the Baltic countries and in northern Europe. Tartu, 2014, 142 p.
54. **Kaupo Mändla.** Southern cyclones in northern Europe and their influence on climate variability. Tartu, 2014, 142 p.
55. **Riina Vaht.** The impact of oil shale mine water on hydrological pathways and regime in northeast Estonia. Tartu, 2014, 111 p.
56. **Jaanus Veemaa.** Reconsidering geography and power: policy ensembles, spatial knowledge, and the quest for consistent imagination. Tartu, 2014, 163 p.
57. **Kristi Anniste.** East-West migration in Europe: The case of Estonia after regaining independence. Tartu, 2014, 151 p.
58. **Piret Pungas-Kohv.** Between maintaining and sustaining heritage in landscape: The examples of Estonian mires and village swings. Tartu, 2015, 210 p.
59. **Mart Reimann.** Formation and assessment of landscape recreational values. Tartu, 2015, 127 p.
60. **Järvi Järveoja.** Fluxes of the greenhouse gases $CO_2$, $CH_4$ and $N_2O$ from abandoned peat extraction areas: Impact of bioenergy crop cultivation and peatland restoration. Tartu, 2015, 171 p.
61. **Raili Torga.** The effects of elevated humidity, extreme weather conditions and clear-cut on greenhouse gas emissions in fast growing deciduous forests. Tartu, 2016, 128 p.
62. **Mari Nuga.** Soviet-era summerhouses On homes and planning in post-socialist suburbia. Tartu, 2016, 179 p.

63. **Age Poom.** Spatial aspects of the environmental load of consumption and mobility. Tartu, 2017, 141 p.
64. **Merle Muru.** GIS-based palaeogeographical reconstructions of the Baltic Sea shores in Estonia and adjoining areas during the Stone Age. Tartu, 2017, 132 p.
65. **Ülle Napa.** Heavy metals in Estonian coniferous forests. Tartu, 2017, 129 p.
66. **Liisi Jakobson.** Mutual effects of wind speed, air temperature and sea ice concentration in the Arctic and their teleconnections with climate variability in the eastern Baltic Sea region. Tartu, 2018, 118 p.
67. **Tanel Tamm.** Use of local statistics in remote sensing of grasslands and forests. Tartu, 2018, 106 p.
68. **Enel Pungas.** Differences in Migration Intentions by Ethnicity and Education: The Case of Estonia. Tartu, 2018, 142 p.
69. **Kadi Mägi.** Ethnic residential segregation and integration of the Russian-speaking population in Estonia. Tartu, 2018, 173 p.
70. **Kiira Mõisja.** Thematic accuracy and completeness of topographic maps. Tartu, 2018, 112 p.
71. **Kristiina Kukk.** Understanding the vicious circle of segregation: The role of leisure time activities. Tartu, 2019, 143 p.
72. **Kaie Kriiska.** Variation in annual carbon fluxes affecting the soil organic carbon pool and the dynamics of decomposition in hemiboreal coniferous forests. Tartu, 2019, 146 p.
73. **Pille Metspalu.** The changing role of the planner. Implications of creative pragmatism in Estonian spatial planning. Tartu, 2019, 128 p.
74. **Janika Raun.** Mobile positioning data for tourism destination studies and statistics. Tartu, 2020, 153 p.
75. **Birgit Viru.** Snow cover dynamics and its impact on greenhouse gas fluxes in drained peatlands in Estonia. Tartu, 2020, 123 p.
76. **Iuliia Burdun.** Improving groundwater table monitoring for Northern Hemisphere peatlands using optical and thermal satellite data. Tartu, 2020, 162 p.
77. **Ingmar Pastak.** Gentrification and displacement of long-term residents in post-industrial neighbourhoods of Tallinn. Tartu, 2021, 141 p.
78. **Veronika Mooses.** Towards a more comprehensive understanding of ethnic segregation: activity space and the vicious circle of segregation. Tartu, 2021, 161 p.
79. **Johanna Pirrus.** Contemporary Urban Policies and Planning Measures in Socialist-Era Large Housing Estates. Tartu, 2021, 142 p.
80. **Gert Veber.** Greenhouse gas fluxes in natural and drained peatlands: spatial and temporal dynamics. Tartu, 2021, 210 p.
81. **Anniki Puura.** Relationships between personal social networks and spatial mobility with mobile phone data. Tartu, 2021, 144 p.
82. **Alisa Krasnova.** Greenhouse gas fluxes in hemiboreal forest ecosystems. Tartu, 2022, 185 p.

83. **Tauri Tampuu.** Synthetic Aperture Radar Interferometry as a tool for monitoring the dynamics of peatland surface. Tartu, 2022, 166 p.
84. **Najmeh Mozaffaree Pour.** Urban Expansion in Estonia: Monitoring, Analysis, and Modeling. Tartu, 2022, 169 p.